THESIS FOR THE DEGREE OF DOCTOR OF PHILOSOPHY

Durability of Cementitious Materials in Long-Term Contact with Water

AREZOU BABAAHMADI

Department of Civil and Environmental Engineering

CHALMERS UNIVERSITY OF TECHNOLOGY

Gothenburg, Sweden 2015

Durability of Cementitious Materials in Long-Term Contact with Water

ISBN 978-91-7597-155-1

Doktorsavahandlingar vid Chalmers tekniska högskola

Ny serie nr 3836

ISSN 0346-718X

Department of Civil and Environmental Engineering

Chalmers University of Technology

SE-412 96 Gothenburg, Sweden
Telephone: + 46 (0)31-772 1000

Cover:
The Calcium Leaching Process: Decalcification of Cementitious Materials

Printed at Chalmers Reproservice AB
Gothenburg, Sweden 2015

TO THE MAN WHO WAS NOT ONLY MY FATHER, BUT A SYMBOL OF STABILITY THROUGH MY LIFE

AND TO THE WOMAN WHO WAS NOT ONLY MY MOTHER, BUT A TRUE ROLE MODEL OF PATIENCE AND UNCONDITIONAL LOVE

TO THEM I OWE MY HAPPINESS

ABSTRACT

Nuclear electricity is considered to be an alternative energy production solution for the power industry in many countries. To ensure the sustainability of this energy solution, the disposal of the produced waste is one of the biggest issues facing nuclear electricity industries. Deep geological disposal of waste with multi-layered engineered barriers has been shown to be one of the safest solutions. However, degradation induced in barrier material by long-term contact with water during the required operational life time of the repository should be accounted for in safety assessments. Cementitious materials are considered to be one of the most efficient alternative barrier materials, providing high pH buffering capacity, good mechanical properties and low diffusivity. The major degradation scenario to consider for these barriers is the dissolution of calcium-containing phases and the eventual leaching of calcium. Decalcification occurs due to the low concentration of calcium ions in the groundwater that comes in long-term contact with the barriers. To facilitate long-term durability predictions, acceleration methods that enhance the calcium leaching process from cementitious materials are needed. However, experimental studies of the natural leaching process under long-term degradation are hampered by the tedious and complicated process of manufacturing large enough decalcified specimens with a composition and pore structure that corresponds to that of concrete leached under natural leaching conditions. In this study, a new acceleration test method for cementitious specimens of flexible size is developed. The electrochemical migration method facilitating both the dissolution and transport of calcium ions provides a higher acceleration rate than other available methods. With application of a current density of 125-130 A/m^2 for 53 days a depletion depth of 75 mm is obtained. The dissolution front, comparable to a natural leaching process, corresponds to the complete leaching of Portlandite, with a certain degree of phase changes in calcium silicate hydrates. The changes in the pore structure, adsorption, ionic diffusion, mechanical strength, elastic modulus, permeability and frost resistance of Ca-depleted concrete, mortar and paste specimens are demonstrated. The results indicate that a considerable increase in pore volume and specific surface area can be expected due to the complete leaching of the Portlandite. This coincides with up to 70% decrease in mechanical strength, more than 40% decrease in elastic modulus and a significant increase in the adsorption capacity and ionic diffusion rates of the leached specimens.

CONTENTS

Acknowledgments

I would like to express my appreciation to my supervisors; Professor Tang Luping and Associate Professor Zareen Abbas, for believing in me and for providing me with their experience and answering my endless flow of questions.

My sincerest gratitude goes to the late Professor Gunnar Gustafson who introduced me to this project. May he rest in peace and his memory remain with us.

I also wish to thank Dr. Per Mårtensson at SKB and Dr. Peter Cronstrand for their constructive comments and suggestions during this work.

I am very grateful to Marek Machowski who always supported me in the lab no matter how busy he was. I am also very thankful to Dr. Helen Johnsson, for all constructive help and advices she gave me. I would also like to thank Dr. Paula Wahlgren, head of the division at Building Technology. I would like to express my gratitude to her specifically for the confidence she gave me in my journey to learn Swedish. My gratitude goes to my colleagues and friends Emma Qingnan Zhang, Vahid Nik and Nelson Silva. This journey would have been impossible without all the great moments I shared with them. All my co-workers and colleagues at the Division of Building Technology are also greatly appreciated for their friendship and all their support.

Special thanks extend to Doctor Katja Fridh at Lund institute of Technology, for her help in frost experiment, Doctor Liu Wei and Liu Jun at Shenzhen University for their help in pore structure measurement.

I am grateful to Mehdi Arjmand not only for the happiness he is in my life, but for the inspiration he is to every PhD student. And last but not least, I would like to thank my parents and my brother for all their love and support during these years of being far from home and my grandmother whose prayers I have always felt with me.

AREZOU BABAAHMADI

Gothenburg, February 2015

ABBREVIATIONS AND NOTATIONS

BET	Brunauer-Emmett-Teller
BJH	Barrett-Joyner-Halenda
C	CaO
C_2S	Dicalcium Silicate
C_3A	Tricalcium Aluminate
C_3S	Tricalcium Silicate
C_4AF	Tetracalcium Aluminoferrite
CH	Portlandite
CSH	Calcium silicate hydrates
DSC	Differential Scanning Calorimetric
EDAX	Energy dispersive X-Ray spectroscopy
EDX	Energy Dispersive X-ray
Ettringite	Calcium Trisulphato Aluminate Hydrate
HCP	hydrated cement paste
IC	Ion Chromatography
LA-ICP-MS	Laser Ablation-Inductive Coupled Plasma-Mass Spectrometry
NMR	Nuclear Magnetic Resonance spectroscopy
S	SiO_2
SEM	Scanning Electron Microscopy
SFL	The final repository for long-lived radioactive waste
SFR	The final repository for short- lived radioactive waste
SKB	The Swedish nuclear fuel and waste management company
TGA	Thermogravimetric Analysis
XRD	X-Ray Diffraction

XRF	X-Ray Fluorescence spectroscopy
LVDT	Linear Variable Differential Transformers
A	Cross-sectional area
c	concentartion
D	Diffusion coefficient
F	Faraday number (C/mol)
I	Current (A)
i	van 't Hoff factor
L	Exposed thickness
m	Mass of substance (g)
M	Molar weight of substance (g/mol)
M	Molarity
n	number of dissociated ions
R	Gas constant (J K^{-1} mol^{-1})
S	Surface area in contact with leachate
T	Absolute Temperature
t	time (seconds)
u	ion mobility
V	Sample volume
z	Valance number of the charged substance
α	degree of dissolution
ΔQ	increase in the specific ions
v_m	velocity of the charged substance
φ	Porosity
Ψ	Electrical potential

PREFACE

The project entitled “Ageing of Cementitious Materials for Storage of Nuclear Waste” was founded by Swedish Nuclear Fuel and Waste Management Company (SKB) and began in August 2010. This work has been carried out at the division of Building Technology, Department of Civil and Environmental Engineering, Chalmers University of Technology. This thesis is based on the following publications, which are referred to in the text by Roman numerals and are attached to this thesis.

PAPER I. A. Babaahmadi, L. Tang, Z. Abbas, Electrochemical Migration Technique to Accelerate Ageing of Cementitious Materials, in: EPJ Web of Conferences, EDP Sciences, 2013, pp. 04002. doi: 10.1051/epjconf/20135604002.

PAPER II. A. Babaahmadi, L. Tang, Z. Abbas, T. Zack, P. Mårtensson, Development of an Electro-Chemical Accelerated Ageing Method for Leaching of Calcium from Cementitious Materials, Materials and Structures, (2015). doi: 10.1617/s11527-015-0531-8.

PAPER III. A. Babaahmadi, L. Tang, Z. Abbas, Ageing Process of Cementitious Materials: Ion Transport and Diffusion Coefficient, in: 3rd International Conference on Concrete Repair, Rehabilitation and Retrofitting, ICCRRR, Cape Town, South Africa, 2012, pp. 369-374. ISBN/ISSN: 978-041589952-9.

PAPER IV. A. Babaahmadi, L. Tang and Z. Abbas, Mineralogical, Physical and Chemical Characterization of Cementitious Materials Subjected to Accelerated Decalcification by an Electro-Chemical Method. The Nordic Concrete Federation. 1/2014. Publication No. 49. pp. 181-198.

PAPER V. A. Babaahmadi, L. Tang, Z. Abbas and P. Mårtensson, Physical and Mechanical Properties of Cementitious Specimens Exposed to an Electrochemical Derived Accelerated Leaching of Calcium. Submitted to International Journal of Concrete Structures and Materials, (2014).

PAPER VI. A. Babaahmadi, L. Tang, Z. Abbas and P. Mårtensson, Long-Term Changes in Physical, Mechanical and Transport Properties of Cementitious Materials Utilized in Nuclear waste Repositories. Submitted to Materials and Structures, (2015).

OTHER RELEVANT PUBLICATIONS BY AUTHOR

i. A. Babaahmadi, L. Tang and Z, Abbas, Physical and Chemical Properties of Cementitious Materials Undergoing Accelerated Decalcification, in: 13th International Conference on Durability of Building Materials and Components, Sao Paulo, Brazil, September 2014.

ii. A. Babaahmadi, L. Tang and Z, Abbas, Chloride Penetration Resistance of Calcium Depleted Concrete Specimens, in: 22nd Nordic Concrete Research Symposium, Reykjavik, Iceland, August 2014, p. 487-490.

iii. A. Babaahmadi, L. Tang and Z, Abbas, Properties of Calcium Depleted Hydrated Cement Paste: Mineralogical Characterization and Cesium Adsorption, in: 2nd International Symposium on Cement Based Materials for Nuclear Waste, Avignon, France, June 2014.

iv. A. Babaahmadi, L. Tang and Z. Abbas, a Study of the Accelerated Ageing Process of Cementitious Materials, in: Advances in Construction Materials through Science and Engineering, Hong Kong, September 2011. RILEM PRO 79 pp. 93.

v. A. Babaahmadi, L. Tang, Z. Abbas and G. Gustafson, Ageing of Cementitious Materials for Storage of Nuclear Waste, in: 21st Nordic Concrete Research Symposium, Hameelinna, Finland, 2011. Publication No. 43 pp. 429-432.

vi. P. Cronstrand, A. Babaahmadi, L. Tang and Z. Abbas, Electrochemical Leaching of Cementitious Materials: an Experimental and Theoretical Study, in: 1st International Symposium on Cement-Based Materials for Nuclear Wastes, 2011. Session 3 (Paper No. O344) pp. 15.

1 Introduction

This chapter provides a background knowledge regarding the importance of the nuclear power industry in many countries as an alternative energy production solution. Consequently, the problems facing the authorities of these countries in managing the disposal of nuclear waste in a sustainable manner are addressed. Accordingly, the assessment of long term functionality of cementitious materials as efficient alternative barriers for nuclear waste repositories is distinguished. Hence, initiation of this research project as a collaboration with the Swedish Nuclear Fuel and Waste Management Company (SKB) to gain a better understanding of the longevity of cementitious barriers is also addressed.

1.1 Nuclear power and waste management

Nuclear power is an important energy production solution for the power industry in many countries. Interest in nuclear power has been revived as a result of concerns about fossil fuel prices, the security of energy supplies and global climate change. According to key world energy statistics provided by the International Energy Agency (IEAE), the top 10 countries with a considerable share of nuclear electricity in their total electricity production are France, Ukraine, Sweden, Korea, United kingdom, the United states, the Russian Federation, Germany, Canada and the People's Republic of China with a share of up to 76% of nuclear electricity in their total domestic electricity production. The IEA assessments show that about 5.7% of the world's energy and 13% of the world's electricity were provided through nuclear power stations in 2012. As reported by Adamantiadesa and Kessides [1], nuclear energy is now a key element in the European Union's climate-change policy. Finland's parliament voted in 2002 to approve building a fifth nuclear power plant, Italy has plans to resume building nuclear plants within five years and Sweden announced plans to overturn a near 30-year ban on new nuclear plant construction. Debates on construction of new nuclear facilities are underway in Germany, Belgium, the Netherlands and Hungary. The demand for nuclear electricity in Asia has also been growing

significantly. A number of countries in East and South Asia: China, Japan, South Korea and India are also planning and building new reactors [1].

Although nuclear electricity is judged as a relatively sustainable energy with a low carbon foot print, the hazards of nuclear power revolve around several basic concerns. The possibility of a nuclear accident is one of the major obvious concerns. However, the developments in safety assessments and the debates regarding legislation can ensure improvements in minimizing production risks. On the other hand, a bigger issue facing the nuclear power industries is the post production phase, such as waste management, which is more complicated as the time scales to deal with are extremely large. As a consequence, a major concern is the lack of comprehensive understanding of permanent and safe disposal of nuclear waste which has been one of the more challenging problems for the nuclear industry [1].

The disposal of radioactive waste is based on the radioactivity level and the life time of the waste. There are four classes of radioactivity for the waste; very low, low, intermediate and high level. Very low level waste is short-lived waste and surface disposal is an option for storing this waste. Low level waste is considered hazardous for few centuries and can be disposed in near-surface disposal facilities with consideration of engineered multi-barriers, depending on the half-life of the waste. The chosen barrier types are: clay, bentonite, quartz sand, graphite, cementitious materials and concrete.

The intermediate and high levels of waste present a hazard for hundreds of thousands of years, and therefore, disposal in a stable geological environment is essential. Such timescales are termed geological because they are characteristic of geological changes of the Earth. In these time durations uncertainties in the risks with near-surface disposal, even if equipped with engineered multi-barriers are very high. Therefore, geological disposal is the only acceptable option [2].

Wet disposal is an option for geological disposal in which the repository is located at a depth of up to 500 m, where eventual water ingress and saturation is inevitable. Various types of host rock are being considered including hard rock (e.g. granite which is being considered in Sweden) and soft rock (e.g. clay in Belgium and France). Considering the direct contact of the facility with water, the role of the engineered barriers in disposal and

storage systems is to ensure the containment of radionuclides and to prevent leachates to the groundwater. However, considering very long-term perspectives in safety prediction, changes in the sealing properties of barriers in direct contact with water is of great importance in the safety analysis.

1.2 Cementitious barriers

Cementitious materials as suitable physical barriers, are efficient chemical binders for waste species and are extensively used in the construction of radioactive waste repositories [3, 4]. These materials which have a high pH buffering capacity, good mechanical properties and low diffusivity are considered as suitable alternative engineered barriers for repositories. The high pH of the pore solution can neutralize the acidity of waste waters and also promote the precipitation of metals. Moreover, because the solubility of carbonates like calcite is lower in high pH levels, the encapsulation of ^{14}C (a radioactive isotope of carbon) can be promoted. However, as mentioned in the previous section, one possible complication is the requirement for long-term service life predictions, which necessitate an accurate demonstration of the changes in functionality of these materials caused by long-term degradations. One of the major promoting factors in degradation scenarios of the barriers is the long-term contact between the barrier materials and the surrounding groundwater [5, 6]. The groundwater surrounding the cementitious barriers in repositories has a different pH and ionic concentrations in comparison with the pore solution of the cementitious materials. The concentration differences will cause ion exchange and interaction and re-depositions of these ions, which will result in the dissolution or precipitation of minerals, and, consequently an alteration in the microstructure and composition of the cementitious materials.

Several researchers have reported investigations into durability analyses of cementitious barriers utilized in repositories of nuclear waste with long-term contact with water [3-42]. However, lengthy perspectives in predictions encounter high uncertainties such as dealing with very complicated and coupled processes that influence the performance of the barriers. Moreover, current knowledge and experimental data about the performance of this construction material does not cover more than a service life of up to 200 years, which is considerably lower than the expected service life for the repositories. This means that there

is not yet sufficient knowledge to demonstrate the effectiveness of these engineered barriers [43], and more assessments are necessary in order to improve the understanding of the long-term performance of such a material.

1.3 SKB

The Swedish Nuclear Fuel and Waste Management Company (SKB), was formed in the 1970s as a partnership between nuclear power companies in Sweden. The organization is tasked to manage the disposal of radioactive waste according to safety regulations from the point that the waste leaves the nuclear power plants.

The current facilities in Sweden include:

- The intermediate storage facility for nuclear fuel (Clab) situated near Oskarshamn
- The final repository for short-lived radioactive waste (SFR) located in Forsmark.

Currently, there are also plans for an extension of SFR and to build a new repository for long-lived radioactive waste (SFL) and a repository for spent nuclear fuel. Spent nuclear fuel, which is considered as long-lived waste, will be deposited in a spent fuel repository. The design of the final repository requires engineered barriers to meet the level of radioactivity of the waste. The current repository for radioactive waste, SFR, consists of several sections with respect to the radioactivity level of the waste, Figure 1-1. These include the Silo (intermediate waste), BMA (intermediate waste), 1BTF and 2BTF (dewatered ion exchange resins) and BLA (low level waste). The facility is a hard rock system located 60 meters beneath the sea. The silo for the most reactive part of the waste is designed with multi-layers of engineered barriers. The waste container is considered to be the first barrier which is embedded in concrete. The reinforced concrete walls provide additional barriers. Furthermore, between the concrete walls and the outer barrier layer of rock, a bentonite layer is engineered providing higher safety. The BMA vault, Figure 1-2, has been designed using rock as the loadbearing parts and in situ casted reinforced concrete is used as the slab and flooring and the walls and the whole structure is constructed on a base of shot rock leveled with gravel. The 1BTF and 2BTF are concrete tank repositories and the BLA vault has a concrete floor and rock walls.

As noted, an extensive amount of concrete is utilized in the construction of the repositories in Sweden. Consequently, safety assessments require predictions regarding the long-term functionality of cementitious barriers in retaining hazardous radionuclides. This motivates the vast amount of research on this topic initiated by this organization.

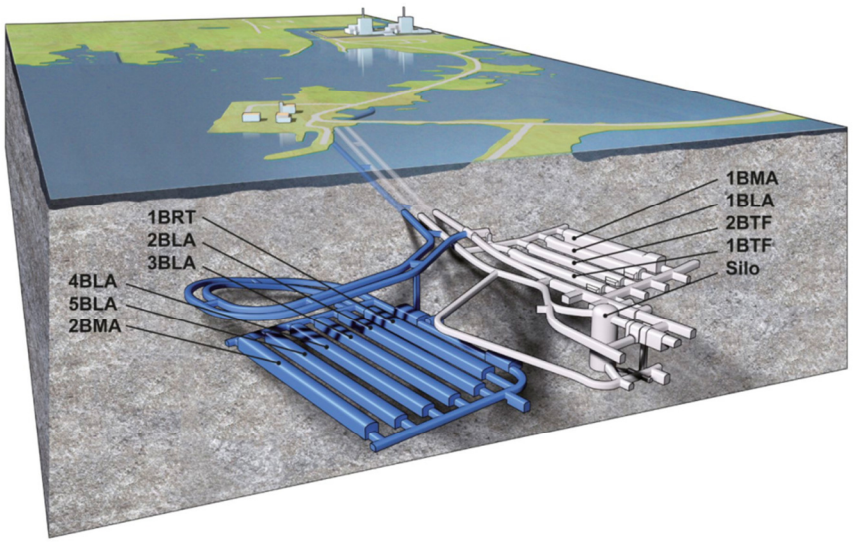

Figure 1-1. Different parts of SFR. The section in blue color is SFR 3 which is planned to be built by 2025

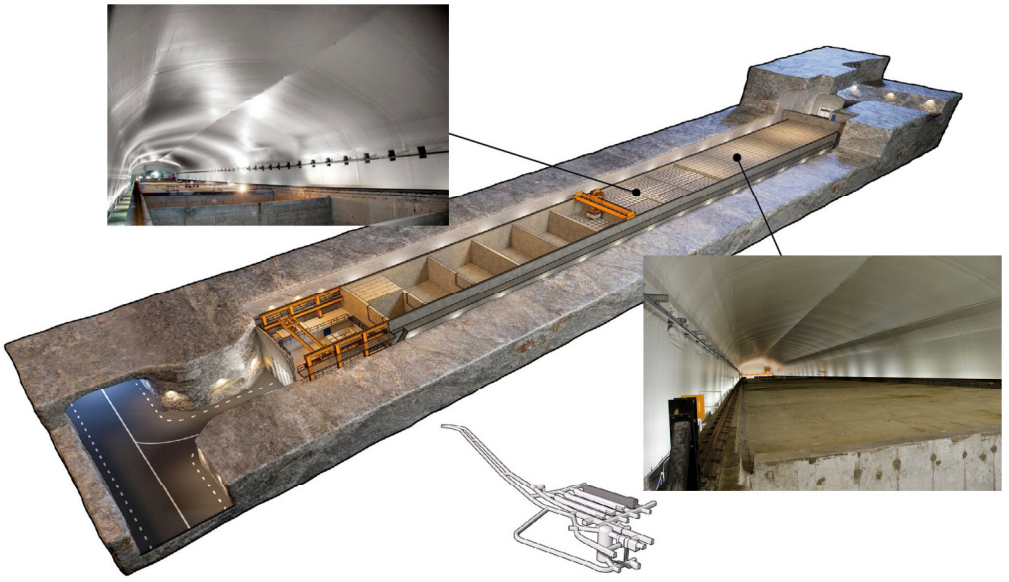

Figure 1-2. The BMA vault: concrete is a major construction material

1.4 Initiation of the project: goals and limitations

In order to broaden the knowledge and understanding of the long-term degradation of cementitious materials as well as to provide databases that account for the changes in the chemical, physical, mechanical and transport properties of the cementitious materials after degradation, a project called "Ageing of cementitious materials for storage of nuclear waste" was initiated and funded by SKB. The major intention was to provide accurate databases for further numerical simulation of the degradation process. The project was defined as a PhD project performed at Chalmers University of Technology, Department of Civil and Environmental Engineering, Division of Building Technology. The primary objectives were to investigate the chemical, physical, mechanical and transport properties of the aged cementitious materials undergoing calcium leaching as the major deterioration factor affecting the cementitious concrete barriers in nuclear waste repositories. The specific goals included in the project description are as follows:

- Laboratory investigation of various aging tests in order to find suitable regimes for manufacturing the aged cementitious materials without significantly distorting the properties of the material from the natural aging processes.

- Development of a proper leaching test method to produce aged specimens of flexible size and comparable to naturally leached specimens, to be used in further tests.

- Laboratory investigation of physical and chemical properties of "young" and aged cementitious materials, including mechanical properties, transport properties (diffusivity), binding (adsorption) capacities, surface complexation (charge) behaviors, and chemical and mineralogical stabilities as well as frost resistance. The predictions should have a perspective of 100,000 years as the service life.

- Synthesis and analysis of the test and modeling results with the intention of establishing a mechanism-based (chemo-mechanical-coupled) model for longevity prediction of concrete for storage of nuclear waste.

It should be noted that chemical degradations and changes in the mechanical characteristics of steel bars in reinforced concrete are beyond the goals of this project. The effect of water cement ratio, mix proportions as well as the utilization of supplementary cementitious materials on durability, are considered as possible future investigations and are not dealt with in this work. It should be noted that the cementitious materials studied in this project were limited to those actually used in repository of nuclear waste in Sweden, SFR.

2 Degradation of Cementitious Barriers

This chapter presents a general knowledge about properties of cement and hydrated cement. A background about durability of cementitious materials and the most important degradation scenarios interfering with long-term functionality of these materials is also presented. Leaching of calcium as a major durability issue is addressed, and test methods for simulating this phenomenon are introduced. Major gaps of knowledge in current understanding concerning changes in properties of cementitious materials are also pointed out.

2.1 Cement and cement hydration

Cement is an essential part of concrete. It hardens after mixing with water through several chemical reactions, and functions as a binder. More than 95% of the cement which is used around the world is Portland cement [43]. The main constituents of Portland cement are calcium oxide (CaO) and silicon dioxide (SiO_2), both of which exist in the Earth's crust as calcium carbonate and sand. Portland cement powder has a grain size between 2 and 80 μm, it is grey in color and has a relative density of about 3.14 g/cm^3. The chemical composition of cement consists of Tricalcium Silicate (C_3S), Dicalcium Silicate (C_2S), Tricalcium Aluminate (C_3A) and Tetracalcium Aluminoferrite (C_4AF), which are known as the four phases of cement. Gypsum is also added to ground clinker in order to regulate the reactivity of the aluminate phases. The Bogue Equation [44] is used to calculate the compound composition of cement . After mixing cement with water, hydration starts. The rate of hardening is very significant after about 2-4 hours and strength is obtained very rapidly after a few days. However, after this time, hardening continues at a decreasing rate for at least a few months. It should be noted that hydration reactions never end, and in order to show the level of reactions, the hydration degree is used as an indicator. The hydration of two phases of cement, C_3S and C_2S, significantly contribute to most of the engineering properties of hydrated cement paste (HCP), like strength and stiffness. The hydration reactions are presented in Equations (2.1) and (2.2) below:

$$2C_3S + 6H \longrightarrow C_3S_2 3H + 3CH \quad (2.1)$$

$$2C_2S + 4H \longrightarrow C_3S_2 3H + CH \quad (2.2)$$

where C is CaO, S is SiO_2, H is H_2O, CH is $Ca(OH)_2$ and CSH is the Calcium Silicate Hydrate.

The aluminate ions in Tricalcium Aluminate (C_3A) and Tetracalcium Aluminoferrite (C_4AF) also react with calcium and sulphate ions to form Calcium Trisulphato Aluminate Hydrate (Ettringite). According to Powers [45] as hydration reactions proceed, more and more anhydrous material is converted into hydrates. This leads to an overall decrease in porosity since the molar volume of hydrates is much larger than that of the anhydrous phases, and the remaining porosity is referred to as capillary porosity.

A major hydration product as stated in Equations (2.1) and (2.2) is Calcium Silicate Hydrate known as CSH gel. The CSH part of HCP is the main phase that contributes to strength properties. The mineralogical structure of the CSH gel is very complex and it is reported to be amorphous to slightly crystalline [46]. It has been shown that CSH has a layered crystal structure similar to tobermorite or jennite, with a layer thickness in the nanometre range [47-49]. The average Ca/Si-ratio is around 1.7 with reported fluctuations between 0.6 and 2 [50]. The CSH layers bear a mixture of $\equiv Si\_OH$ and $\equiv Si\_O^-$ groups. The proportion of O groups increases as the Ca/Si ratio and the pH increase [50]. Thus, the CSH layers are negatively charged particles, although because of the high concentration of calcium ions a charge reversal may occur [50]. However, the structure of the CSH gel accommodates available adsorption sites and high specific surface area, which has a direct influence on the diffusion/adsorption properties of cementitious materials [51].

The CH known as Portlandite is the main crystalline part of the HCP. It provides alkaline characteristics (pH: 12.5-13) which have a great influence on the durability of cementitious materials. Figure 2-1, illustrates the main constituents of HCP after a few weeks of hydration. As illustrated in this figure, the hydrated cement matrix contains water-filled gaps which are known as pores. The volume of the pore structures depends on the water cement ratio. The magnitude of the pore volume has a direct influence on the strength as well as the transport properties of the cementitious materials. There are two types of pores

in the HCP system: capillary pores and gel pores. The usual pore size categorization is interlayer pores (2nm), gel pores (2-10 nm) and capillary pores (10 nm-5 μm) [46]. There are also air voids in the system with sizes ranging on the scale of 5 μm-5 mm.

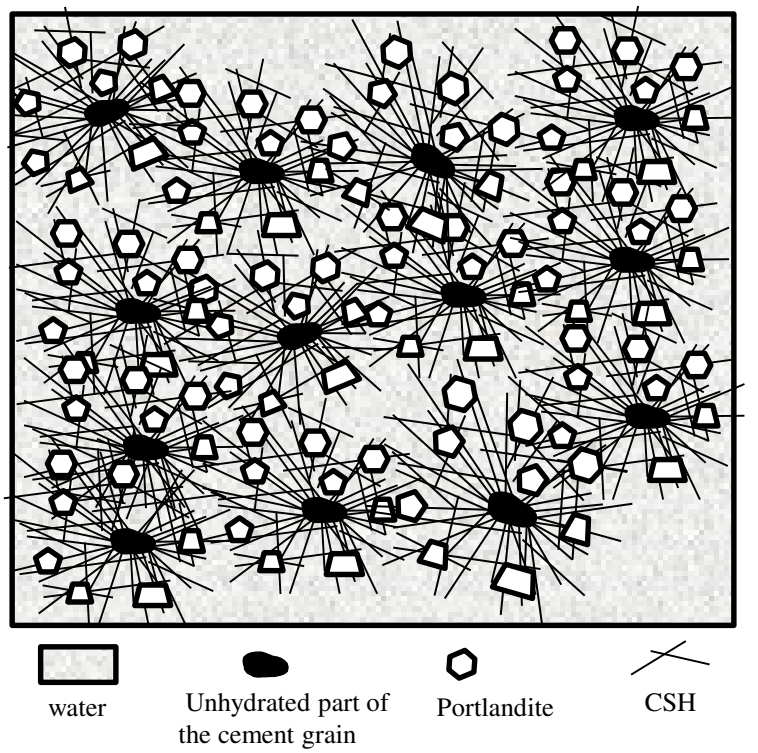

Figure 2-1. The main constituents of HCP after a few weeks of hydration

2.2 Degradation scenarios

The interactions between the cementitious materials and the surrounding environment encounter changes in these materials. The exchange of ions between the environment and the hydrated cement paste, and the interaction and re-deposition of these ions would cause alterations to the properties of cementitious materials. Moreover, changes in surrounding climate conditions (high temperature gradients and freeze-thaw) are other important factors that can influence the durability of cementitious materials.

2.2.1 Chloride ingress

One well-known scenario concerning the service life of specifically reinforced concrete structures is chloride ingress. The exposure of cementitious materials to chloride ions will

cause a reaction with aluminate phases in the paste and the formation of Friedel's salt ($3Cao.Al_2O_3.CaCl_2.10H_2O$) [52-55]. The production of other solid phases such as Kuzel's salt (Chloro-sulfate AF_m) [56] and calcium oxychlorides [52] has also been reported in the literature. The production of these solid phases might cause expansion and cracking, but these new solid phases are not readily produced after the penetration of chloride ions. The interaction of chlorides and the HCP matrix is not necessarily a chemical interaction that leads to the formation of new solid phases as soon as the exposures are taking place. That is because the early exposure interactions in the pore solution of cementitious materials are affected by binding phenomena [57, 58]. The overall amount of chlorides that react with the materials in early chloride exposure has also been taken into consideration in the investigation by Tang and Nilsson [59].

Moreover, it has been reported that the chloride concentration of the groundwater around repositories is too low to form Friedel's salt (<0.1 M [60]). This indicates that formation of Friedel's salt is not considered as a leading degradation scenario when dealing with safety assessments of cementitious barriers.

A chloride intrusion may indirectly influence the concrete barriers due to initiating steel corrosion in reinforcements. Corrosion products are expansive and will lead to eventual cracking and distortions. The major effect of the presence of chlorides is the destruction of the protective passive layer on the steel reinforcement surface causing the initiation of corrosion [61]. The corrosion products contribute to stress around the rebar, and consequently damage the concrete cover.

2.2.2 Carbonation

Another well-known source of degradation in cementitious systems is carbonation. If gaseous carbon dioxide penetrates in to the HCP matrix it will cause the production of HCO_3^- and CO_3^{2-} which will react with dissolved calcium, and this reaction will lead to the precipitation of $CaCO_3$ (Calcite). Although the production of calcite causes a reduction of material porosity and increases the retention of the HCP constituents [29], the consumption of Portlandite causes a pH drop in the system. The pH drop can affect the protective passive layer of the reinforced steel. This will initiate steel corrosion. Moreover, carbonation might also cause changes in the solubility of the HCP constituents [29, 62].

2.2.3 Sulfate attack

Sulfate attack is another degradation problem. The reaction of sulfate ions with the HCP phases leads to the production of:

- Gypsum ($CaSO_4.2H_2O$),
- Ettringite ($[Ca_3Al(OH)_6{\cdot}12H_2O]_2{\cdot}(SO_4)_3{\cdot}2H_2O$) and
- Thaumasite ($Ca_3[Si(OH)_6{\cdot}12H_2O]{\cdot}(CO_3){\cdot}SO_4$).

These products can cause expansion, spalling and severe degradation [63-65]. The source of sulfate ions is usually the groundwater surrounding the cementitious barriers, and since the pH level is commonly near neutral in these environments, the sulfate ingress will be accompanied by leaching [4]. This emphasizes the importance of coupling the effect of sulfate attack with leaching phenomena when dealing with safety assessments.

2.2.4 Leaching of calcium

Another factor behind major deterioration in the long-term service life of cementitious barriers in a nuclear waste repository is the leaching of calcium [5, 6]. The low calcium content of the water in the surrounding environment causes a concentration gradient which leads to dissolution and eventually the leaching of the calcium from the hydrated cement matrix. It has been mentioned earlier that CSH and CH parts of the HCP system contribute to strength and durability properties, and therefore, decalcification affects the chemical and mechanical properties of the cementitious materials. The dissolution of the CH part of HCP encounters extreme changes in the pore structure which leads to changes in transport regimes and strength properties [12, 17, 22, 27, 36]. The induced calcium depletion will also lead to changes in the surface charges of CSH and eventually the surface area, which will have an extensive effect on the adsorption properties of the cementitious systems [17]. The coupled chemical/physical and mechanical changes might induce changes in freeze-thaw properties as well. It should be noted that this degradation process is relatively slow, but will be magnified from the service-life perspective of nuclear waste repositories.

Figure 2-2 briefly illustrates the influencing degradation factors and the consequent encountered degradations.

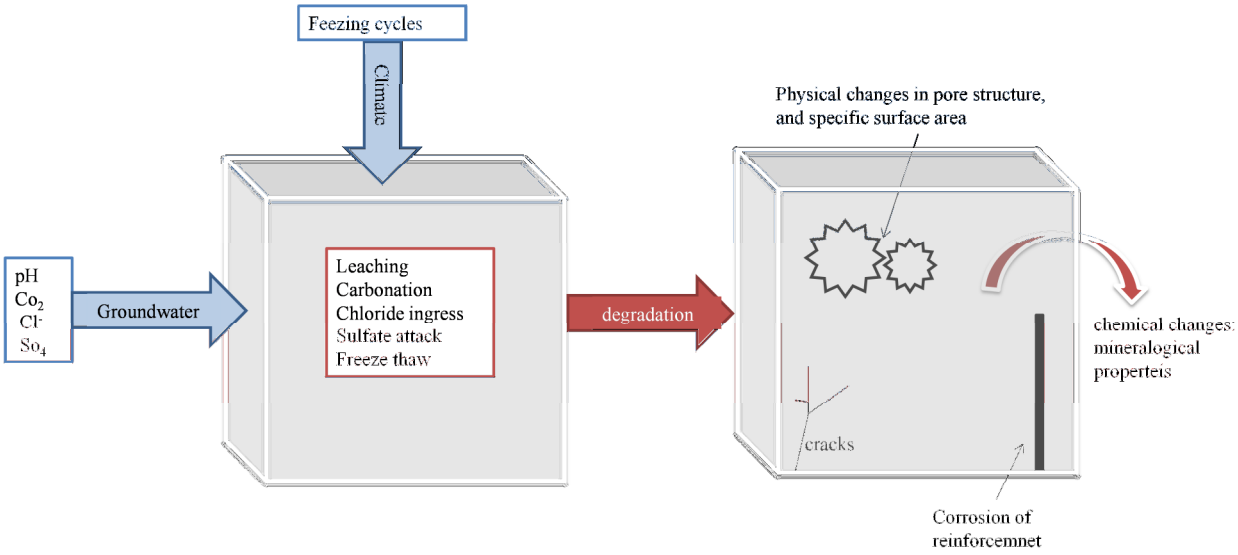

Figure 2-2. Degradation of cementitious materials

Of all the major degradation scenarios for cementitious materials, calcium leaching is often stated as the major degradation scenario of cementitious materials in long-term contact with water [5, 6]. Moreover, the other degradation processes, such as chloride and sulfate ingress as well as carbonation, are extensively affected and coupled with the leaching phenomena. This motivates the importance of considering the coupled effect of leaching on other degradation processes while drawing conclusions in safety assessments.

2.3 Experimental simulation of decalcification process

As explained in the previous section, a major process that causes the degradation of cementitious materials in long-term contact with water is the decalcification of the hydrated cement system. It has been shown in several studies that the calcium leaching process is governed by a coupled dissolution/diffusion process [66]. By definition, leaching is the removal of a soluble phase, in the form of a solution, from an insoluble permeable solid.

The kinetics of an ionic diffusion process are presented in a simplified way in Equation (2.3) [8].

$$\phi(x,t)\frac{\partial c(x,t)}{\partial t} = D(x,t)\frac{\partial^2 c(x,t)}{\partial x^2} - \frac{\partial c_s(x,t)}{\partial t} \qquad (2.3)$$

where, $c(x,t)$ is the Ca^{2+} concentration in the liquid phase, $c_s(x,t)$ is the content of Ca^{2+} in the solid phase, $\phi(x,t)$ is porosity and $D(x,t)$ is the diffusion coefficient.

Although this equation is rather simplified (the influence of phenomena such as chemical activity, electrical coupling and convection is neglected), it indicates that a major factor in a diffusive transport process is the concentration gradients. Due to a low concentration of calcium ions in the water, the dissolution of calcium hydroxides followed by the diffusive transport of calcium ions, or leaching of calcium, occurs. The loss of calcium leads to the dissolution of Portlandite followed by the decalcification of CSH. Figure 2-3, illustrates the simplified decalcification process of HCP.

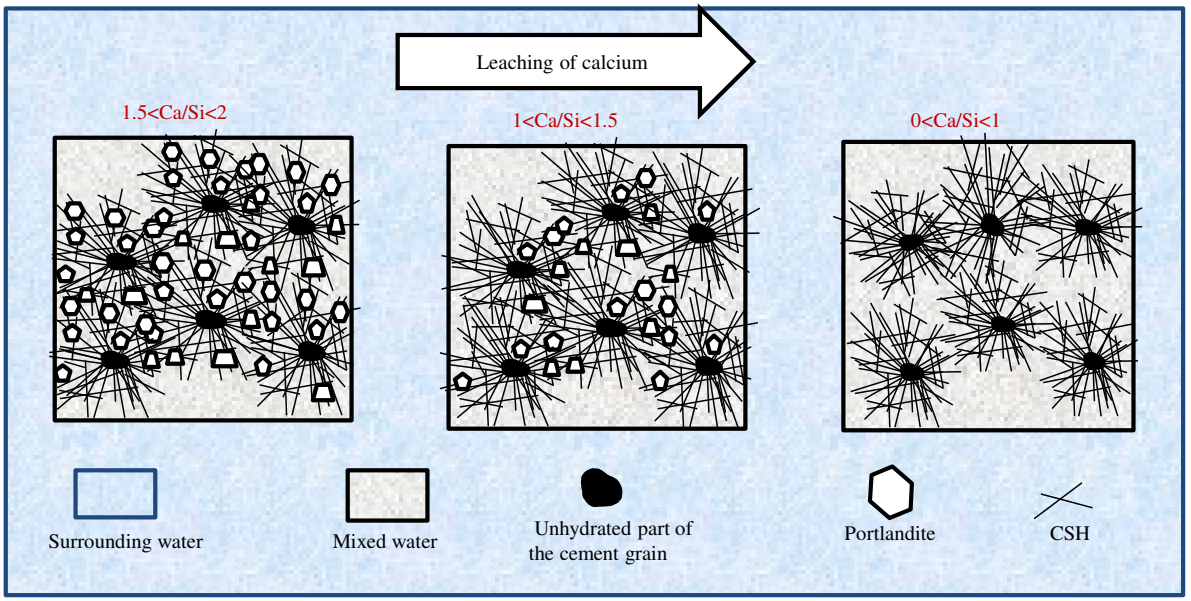

Figure 2-3. Decalcification of hydrated cement paste

A more complex model that describes the process should consider all the possible dissolution/precipitations, adsorption/desorption and cation exchanges. Since the process frequently encounters changes in the properties of the solid matrix, the effect of the continuous changes on leaching propagation should also be considered.

As decalcification phenomenon is relatively slow, usual structures such as tunnels, bridges or even dams which have shorter required service life compared to repositories cannot show the severity of the degradation induced by long-term leaching of calcium. Several standard test methods have been developed to provide adequate information for regulating acceptable thresholds for dealing with nuclear waste safety assessments. The ANS 16.1,

ASTM C1308 [67, 68] as well as parallel batch extraction test, up-flow percolation column and tank leaching tests [69] are some examples. The test methods are either kinetic-based to measure specific diffusion coefficients or equilibrium-based to account for the characteristics of the barrier and surrounding environment in equilibrium [4]. The batch reaction test is based on the application of acidic or basic solutions on solid materials with reduced particle size. The percolation column utilizes the effect of an advective flow and the tank leaching test is an immersion test with frequent exchanges of the leaching solution [4]. Several other improvised versions of these test methods have been reported in literature, which simply induce the leaching process through the immersion of solid cementitious materials in leaching solutions. [7, 11, 13, 21, 22, 26, 27, 30, 31, 37, 42, 70-72]. The reduced solid particle size and also the chemical properties of the leaching solutions (pH and ionic concentration) introduce acceleration rates in the leaching process in some of the proposed test methods. Since this is a matter of a very slow process, more accelerated leaching test methods with high acceleration factors have been developed in order to draw conclusions about long-term predictions and in order to avoid extrapolating short term data sets. These methods either utilize electrical field [11, 13, 70, 73] or aggressive leaching solutions [26, 37, 74] to change the kinetics of the process.

2.3.1 Accelerated calcium leaching test methods

2.3.1.1 Electrical acceleration

A well-known acceleration method is electrical migration. There are a few studies in the literature based on the migration concept [11, 13, 70, 73]. According to the definition of migration, it is possible to move charged substances with the application of an electrical field. The charged substances move under the gradient of the electrical field in a certain direction according to their valance state. The average velocity of the movement is defined according to Equation 2.4.

$$\upsilon_m = u \cdot \frac{\partial \psi}{\partial x} \tag{2.4}$$

Where, υ_m is the velocity of the charged substance and u is the ion mobility.

According to the Einstein relation, ion mobility can be defined as Equation (2.5).

$$u = D \cdot \frac{z \cdot F}{R \cdot T} \tag{2.5}$$

where, D is the diffusion coefficient, z is the valance number of the charged substance, F is the Faraday number equal to 96485 C/mol, R is the gas constant and T is the temperature.

The actual movement of ionic species can be described by the Nernst-Plank Equation:

$$J_i = -D_i \frac{\partial c_i}{\partial x} - c_i D_i \frac{z_i F}{RT} \cdot \frac{\partial \Psi}{\partial x} \tag{2.6}$$

where J is the flux of ions, D denotes the diffusion coefficient, c is the molar concentration, R is the gas constant, T is the absolute temperature, x is the distance, z is the valence of ions, F is the Faraday constant, and Ψ is the electrical potential including both the so-called counter electrical potential caused by different mobilities between anions and cations and the imposed external electrical potential across the anode and the cathode. The subscript i represents a specific type of ions. On the right side of Equation (2.6), the first term describes diffusion, while the second term describes the migration process. Equation (2.6) has been used by Tang [75] in the development of the rapid chloride migration test which was adopted as the Nordic standard NT BUILD 492 [76].

Under a certain gradient of external electrical potential, the migration current is the sum of ions moving in the pore solution that is shown in Equation (2.7):

$$I = AF \sum_j z_j J_j = AF \sum_j z_j \left(- D_j \frac{\partial c_j}{\partial x} - c_j D_j \frac{z_j \quad F}{RT} \cdot \frac{\partial \Psi}{\partial x} \right) \tag{2.7}$$

where I is the migration current and A is the cross-sectional area of the specimen. The subscript j denotes various types of ions. Combining Equations (2.6) and (2.7), one can obtain Equation (2.8):

$$J_i = -D_i \frac{\partial c_i}{\partial x} + \frac{D_i z_i c_i \left(\sum_j D_j z_j \frac{\partial c_j}{\partial x} + \frac{I}{AF} \right)}{\sum_j D_j z_j^2 c_j} \tag{2.8}$$

A more detailed description of the electrochemical migration theory has been presented by Cronstrand et al. [77].

There are very few reported migration-governed accelerated leaching test methods in the literature. The methods entail the utilization of an electrical cell, in which the cementitious specimen is a porous barrier through which ions can migrate due to induced electrical gradients. In a study performed by Saito et al. [11], a disc of a mortar sample with a diameter of 50 mm and a thickness of 10 mm was placed between two glass vessels containing water as the electrolyte. A constant potential of 25 V was applied during the experimental time and carbon electrodes were used as the cathode and the anode. Ryu et al. [13], had utilized titanium mesh as the electrode and water is the electrolyte. The electrical cell was designed in such a way that catholyte and anolyte solutions were in contact, as the specimen with an embedded electrode (anode) was immersed in water in a container. The cathode was also placed at the bottom of the container. A low current density of 10 A/m^2 was applied because of the low dissolution rate of calcium ions.

2.3.1.2 Application of ammonium nitrate

Another category of accelerated leaching is the application of aggressive solutions. A well-known chemical acceleration method presented in the literature is the immersion of samples in a concentrated ammonium nitrate solution [26, 37, 74]. As reported by Heukamp et al. [26] as well as Carde [37], the application of ammonium nitrate solution favors the dissolution of calcium hydrates because of the formation of highly soluble $Ca(NO_3)_2$ along with the consumption of the OH^- ions in calcium hydroxides. However, it should be noted that due to the low concentration of calcium ions in pore solution, $Ca(NO_3)_2$ can only exist as ions of Ca^{2+} and NO_3^- and precipitations of this product will not exist. This indicates that the presence of nitrate ions in the pore solutions is major the factors facilitating the dissolution of calcium hydroxides.

In this method, cylindrical paste specimens with the size of Ø11.5×60 mm were immersed in an oscillating box containing 6 M ammonium nitrate solution. In order to reach a quasi-steady state, 45 days of experimental time was required, and during this time the propagation of the dissolution front was $2mm/\sqrt{day}$. Other test set-ups utilizing specimens of different sizes with different experimental durations have also been reported in the

literature. Nguyen et al. [18] have reported on the application of specimens of the size Ø32×100 mm and Ø110×220 with an experimental time of up to 547 days. Choi and Yung [35] have used cylindrical concrete samples of the size Ø100×100 mm and an experimental time of up to 365 days.

2.3.2 Reported properties of decalcified cementitious materials

The test methods and standards noted in previous sections were developed to account for the properties of calcium-leached cementitious materials. A study by Adenot [42] has demonstrated that the degraded material has a layered system which consists of different zones separated by precipitation/dissolution fronts and progressive decalcification of CSH. The secondary precipitation of Ettringite and AFm (Alumina Ferric Oxide Monosulfate) and calcite has also been reported [31].

It is also reported that leaching front is characterized by continuous decalcification of the CSH phase with a gradient of Ca/Si-ratio between the sound and leached zone. This causes silicate polymerization and as a result several adsorption sites become available on the CSH surface. The presence of these sites could cause the incorporation of dissolved iron or aluminum in the CSH matrix [30, 31].

It is also demonstrated that the changes in pore structure are attributed to the leaching of Portlandite. In addition, it is shown that for larger initial Portlandite content, the magnitude of the changes in pore volume is also larger [27]. It has also been reported that the induced increase in porosity caused by the degradation of the CSH gel is very low and can be neglected [22, 27, 36]. Moreover, several investigations have demonstrated the effect of changes in pore volume on strength properties [12, 18, 35, 36]. Although the results of these studies showed considerable deviations, all of the investigations indicated that lower mechanical strength is a result of larger pore volume. In addition, changes in the surface charges of the CSH gel due to silicate polymerizations, causing changes in adsorption properties are reported as well [17]. More available adsorption sites mean a higher available specific surface area as well.

2.3.3 Complications and gaps in knowledge

As noted in previous sections, there are a vast number of test methods that are reported in the literature to experimentally simulate the calcium leaching process. One complication is that test methods that approximate natural leaching conditions are very time consuming because the leaching process is very slow. Moreover, even if using acceleration to facilitate the process, an accelerated leaching test might not properly simulate the process. In addition, the available accelerating laboratory test methods use relatively small sample sizes to reach higher acceleration rates. This indicates that accurate further testing of properties such as transport, frost or mechanical strength, is not possible. Also, because leaching is a dissolution/diffusion governed process, high acceleration rates can be achieved if both dissolution and diffusion phenomena are accelerated. However, the electrical acceleration methods can only accelerate the ionic transport process by introducing migration instead of diffusion, but the kinetics of the dissolution process will not be changed. On the other hand, chemical acceleration with leaching solutions, such as high concentrations of ammonium nitrate, accelerates the dissolution process while the ion transport remains slow and diffusion-governed.

It should be noted that a proper acceleration method should not create an over-estimation in the simulation of a natural process. Nevertheless, the proposed electrical leaching test methods cause degradation due to the production of H^+ ions close to the anode. The acidic characteristic of this ion cause unrealistic degradation in the specimens. As reported by Saito et al. [11], a Ca/Si-ratio of zero can be obtained after less than 500 days of leaching with an electrically accelerated test method. This indicates that severe degradation will be obtained in less than 2 years, which is an extreme over-estimation. In addition, the application of a highly concentrated ammonium nitrate might cause inhomogeneous accelerated leaching due to excessive degradation on the surface of specimens in direct contact with the aggressive solution.

Consequently, a test method accelerating decalcification for specimens of flexible size that speeds up both the dissolution and diffusion processes with the least amount of over-estimation is needed to better demonstrate the circumstances of decalcification. The produced electrochemically aged specimens should be thoroughly characterized to enable a comparison with naturally aged specimens.

3 Methods and Experimental Details

In order to attain the goals within the scope of this project as well as considering the importance of an efficient test method for calcium leaching as demonstrated in the previous chapter, the experimental approach in this project was prioritized as follows:

I. Development of an accelerated leaching test method for cementitious specimens of flexible size.

II. Demonstration of the comparability of the produced aged specimens with leached samples produced through reference leaching test methods proposed in the literature.

III. Investigation of the changes of the properties of the age specimens caused by leaching. The considered properties are: transport properties, diffusion/adsorption, mechanical strength, frost resistance as well as physical properties such as permeability and pore structure changes.

This chapter presents all the experimental approaches and the details of the performed test methods to achieve the above-mentioned goals. The chapter starts by presenting the preparation procedures for all the cementitious specimens used in the test methods. Then, the electrochemical migration test method as the main focus of the project is presented. Thereafter, the set-up designs of all the performed reference leaching test methods formulated according to literature propositions are demonstrated. Details of instrumental analyses and characterization of leached specimens are also presented.

3.1 Specimen preparation

The paste specimens were cast from a mixture of Swedish structural Portland cement for civil engineering (CEM I 42.5N SR3/MH/LA) and deionized water at a water-cement ratio (W/C-ratio) of 0.5. The chemical composition of the cement is listed in Table 3-1. Fresh cement paste was cast in acrylic cylinders with an internal diameter of 50 mm and a length of 250 mm. The ends of the cylinders were sealed with silicone rubber stops. The cylinders containing fresh paste were rotated longitudinally at a rate of 12-14 rpm for the first 18-24

hours of hydration in order to produce specimens with a homogeneous composition and structure. Afterwards, the rubber stops were removed and the ends of the cylinders were sealed with plastic tape. The specimens were stored for over 6 months in a tight plastic box, and then cut into cylinders with the size of Ø50×75 mm for use as specimens in the experiments. In order to prevent carbonation, saturated lime water was used at the bottom of the plastic box as an absorbent for carbon dioxide during the storage of specimens. To further ensure that the specimens used in the leaching experiments were not carbonated, the paste portions about 10-20 mm from the ends of the cylinders were cut off prior to specimen cutting. The initial calcium and silica content in hydrated cement is calculated and presented in Table 3-2.

Table 3-1. Chemical composition of Swedish CEM I 42.5N SR3/MH/LA.

Chemical formulation	**CaO**	**SiO_2**	**Al_2O_3**	**Fe_2O_3**	**MgO**	**Na_2O**	**K_2O**	**SO_3**	**Cl**
Percentage	64	22.2	3.6	4.4	0.94	0.07	0.72	2.2	0.01

Table 3-2. Initial calcium and silica contents in a cement paste specimen (Considering $C_3S_2H_3$ as the composition of CSH)

Total	**Component**	**mole/gr paste**	**Ca/Si (in mole)**
Calcium content	CSH	0.0044	**3.1**
	CH	0.003	
	Other hydrates	0.0018	
	Total	0.0092	
Silica content	CSH	0.003	

The mortar specimens at a W/C-ratio of 0.5 and a cement:sand-ratio of 1:2, were cast from mixtures of Swedish structural Portland cement for civil engineering (Table 3-1), deionized water and natural sand with a maximum particle size of 1 mm. A casting procedure similar to the one for paste specimens was followed.

The concrete specimens were cast from mixtures of Swedish structural Portland cement for civil engineering (Table 3-1), natural sand and crushed coarse aggregate with a maximum size of 16 mm. The specimens were cast in cylinders in two different dimensions of Ø100×200 mm and Ø50×250 mm with two different W/C-ratios (in line with the properties of the concrete used in, SFR, in Sweden [33, 78]), Table 3-3. The slump of fresh concrete prior to casting was 25 mm for the concrete with W/C=0.48 and 35 mm for W/C=0.62. The specimens were cast in cylinders in two different dimensions of Ø100×200 mm and Ø50×250 mm. 24 hours after casting, the specimens were demolded and cured in the saturated lime water for more than 3 months in a moist plastic box and then cut to cylinders with the dimensions of Ø50×75 and Ø100×50 mm to be used in the leaching experiments.

Table 3-3. Properties of concrete used in SFR repository located in Forsmark, Sweden.

Properties	**Silo[1]**	**BMA[2]**
Cement type	Swedish structural cement	Swedish structural cement
W/C	0.48	0.62
Cement content (kg/m^3)	350	300
Aggregate volume fraction[3]	0.7	0.7

[1] Based on Emborg et al. [33], however with a symmetrical deviation of 48±5 MPa in compressive strength instead of 43-58 MPa with a mean 48 MPa.

[2] BMA: rock vault for intermediate level radioactive waste. The data has been estimated based on the previous Swedish concrete class K30.

[3] Estimated based on the general mix design of concrete mix proportion, which is in line with Höglund [78] for the concrete in silo.

3.2 Electrochemical acceleration method

As mentioned in the previous chapter, although some important conclusions have been drawn in several studies reported in the literature regarding the chemical properties of Ca-depleted materials, in particular, the test methods available in the literature have been limited to the use of crushed materials or small solid samples. This has limited the possibilities to properly study the mechanical and physical properties of cementitious materials, e.g. compressive strength and diffusivity, which require the use of larger

samples. In addition, not many studies reported in the literature cover the implications of concrete specimens of proper size but instead paste specimens or powder samples have been used. Moreover, the proposed acceleration methods in previous studies did not accelerate both processes (dissolution/diffusion) governing the leaching phenomenon, which, consequently limits the obtained rates of acceleration. Further, as also noted in Section 2.3.3, the methods in previous studies have not entirely simulated the natural situation because of the introduction of some over-estimations and undesired degradation scenarios. For this reason, an efficient accelerated leaching method for the decalcification of cementitious materials of the proper size, is developed in this project. The electrochemical migration method:

- enables acceleration of both dissolution and diffusion processes governing the leaching phenomenon and consequently a high leaching rate of calcium,
- allows application of specimens of flexible sizes,
- enables homogeneous leaching of calcium, and
- prohibits degradations caused by extensive over estimated decalcification.

The initial set-up design of the method was regulated according to literature recommendations. However, the initial design was gradually refined in order to achieve the most efficient combination of adjustable settings that enabled the leaching of calcium without causing unexpected damage to the specimens. The adjustment of several set-up parameters was based on the results and observed outcomes from a series of experimental trials. A complete demonstration of the gradual refinement of the method development process can be found in a licentiate thesis by Babaahmadi [79]. Paper I, presents some concluding remarks based on a pre-developed version of the method. The results presented in Papers II, IV, V and VI, are based on the finalized set-up design of the method. A step-by-step experimental procedure for an electrochemical acceleration method is presented in Appendix.

3.2.1 Set-up design

The set-up design of the electrochemical migration method was based on the rapid chloride migration method developed by Tang [75], Figure 3-1. However, this method was re-adjusted, thus enabling accelerated leaching of calcium from cementitious specimens. The

design included utilizing a cementitious specimen which was placed between two electrolyte solutions (electrical cells) as a porous medium for ion migration. The sealant was asphalt tape which is 2-3 times longer in height than the specimen's, and provided an empty volume of about 250 ml used as the anolyte container. A plastic box with the capacity of 30 liters was used as the catholyte container. The cathode was made of stainless steel and was mounted on a plastic support in a similar way as described in NT BUILD 492 [76]. The anode was produced using a titanium mesh and was equipped with a plastic spacer that prevented direct contact with the specimen.

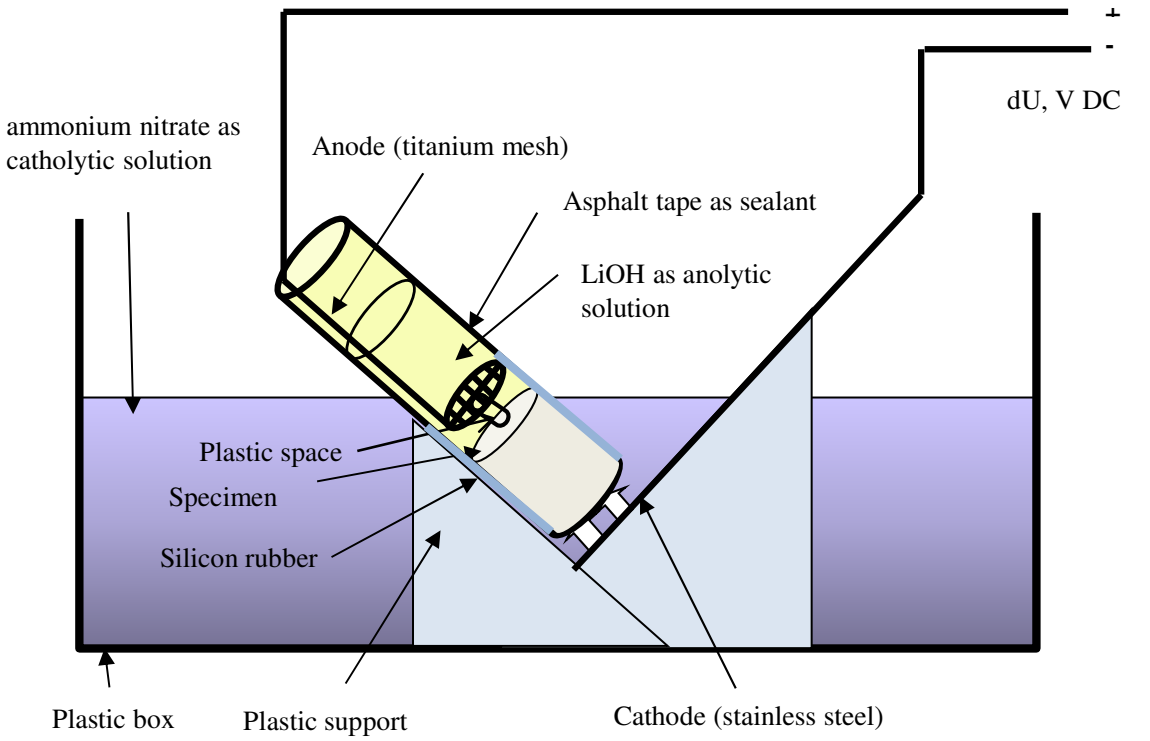

Figure 3-1. Set-up design for electrochemical migration method

3.2.1.1 Anolyte/Catholyte solutions

The electrolyte solutions were selected in a way to minimize the undesired destructive scenarios which exist in some other proposed acceleration methods and also to accelerate dissolution processes. It was noted in the previous chapter that the application of ammonium nitrate to accelerate the dissolution of calcium-containing phases has been reported in literature [26, 38]. However, although the dissolution of calcium is enhanced according to these studies, the transport of nitrate ions into the pore solution as well as the

leaching of calcium is still very slow due to the slow diffusion process. On the other hand, with the application of an electrical gradient, a homogeneous transport process of nitrate ions as well as higher leaching rates of calcium can be achieved. Consequently, an ammonium nitrate solution was used as the catholyte solution in the electrochemical migration method to obtain the combined effects of both chemical and electrical acceleration. Moreover, as mentioned in the previous chapter, the applied high concentration of this solution (6 M), results in an overestimated concentration gradients, which might cause magnified decalcification in the surface of exposed specimens. To prevent such degradations, a concentration close to the ionic concentration in the pore solution of the specimen was selected in this study. Assuming that the pH level in the pore solution is approximately 13.5, a concentration of 0.3 M was chosen.

Also, as stated in the previous section, a major problem with electrical acceleration is the induced H^+ ions produced at the anode. The acidic characteristics of these ions results in severe magnified degradations (Saito et al. [11] have reported that a Ca/Si-ratio = 0 can be achieved in less than 2 years of experimental time). To avoid this phenomenon, a lithium hydroxide solution was chosen as the anolyte solution in the electrochemical migration method, because the hydroxide ions will neutralize the produced H^+ ions. Also, since Li^+ ions are not present in the pore solution of the cementitious specimens, these will not interfere with leaching of the existing ions in pore solution. Moreover, Li^+ ions with a crystallographic radius of 0.07 nm have a high surface charge density, and therefore they are strongly hydrated in water and acquire a large size [80]. Therefore, the thick water layer around Li^+ in a solution will reduce the tendency for diffusion or migration of Li^+ ions.

To use nitrate as the negative ions and to reduce the amount of free OH^- ions in the catholyte solution, ammonium nitrate was added to the catholyte. In the catholyte, ammonium was in equilibrium with ammonia, Equation (3.1), and the pH level was below 9, which means that the H^+ will neutralize the OH^- formed at the cathode.

$$NH_4^+ \leftrightarrow NH_3(aq) + H^+ \tag{3.1}$$

As the amount of free OH^- ions were reduced in line with the process described above, the nitrate ions became the dominant negative ions for migrating into the specimen, and this

facilitated the dissolution of the Portlandite and kept the specimen under a low resistivity for a longer experimental time, as shown in Trial 3 in Figure 3-2. The figure illustrates that with the application of ammonium nitrate, the resistances decrease in time while when using only deionized water as the catholyte, the leaching stops after about 150 hours. A plausible explanation for this behavior is that when the initial alkaline ions K^+ and Na^+ in the pore solution leach out, there should be an agent that favors the dissolution of Portlandite so that the leaching can be followed by calcium migration. However, when using deionized water as catholyte solution, low availability of calcium ions (due to low solubility of Portlandie) after a certain time of leaching cause high resistances. On the other hand, when utilizing ammonium nitrate, since the nitrate ions enhance dissolution of Portlandie, dissolved calcium ions would be available for continuation of the leaching process. Consequently, with application of ammonium nitrate solution as catholyte, the resistance inside the specimen will not increase.

3.2.1.2 Current or potential range applied to the specimen

In order to avoid any temperature-induced mechanical destruction of the specimen, the current applied to the specimen was controlled and kept constant to prevent any significant elevation in temperature caused by the Joule Effect. The application of a constant current also enabled accounting for the exact amount of electrical charge (Coulombs) through the specimen.

As mentioned in the previous chapter, low current densities are reported to be utilized in the electrical acceleration methods proposed in the literature (10 A/m^2 as reported by Ryu et al. [13] and 36 mA/m^2 as reported by Castellote et al. [73]). This is due to the low dissolution rates of the calcium-containing phases which lead to high resistances. However, by applying ammonium nitrate to increase the dissolution kinetics, it is possible to use higher current densities without any temperature-induced degradation in the specimen. Here, a current density of 125-130 A/m^2_{paste} is proposed in the electrochemical migration test method. According to the pilot scale experiments, the temperature fluctuates in the range of 20-30 °C, which would not cause any temperature-induced cracking.

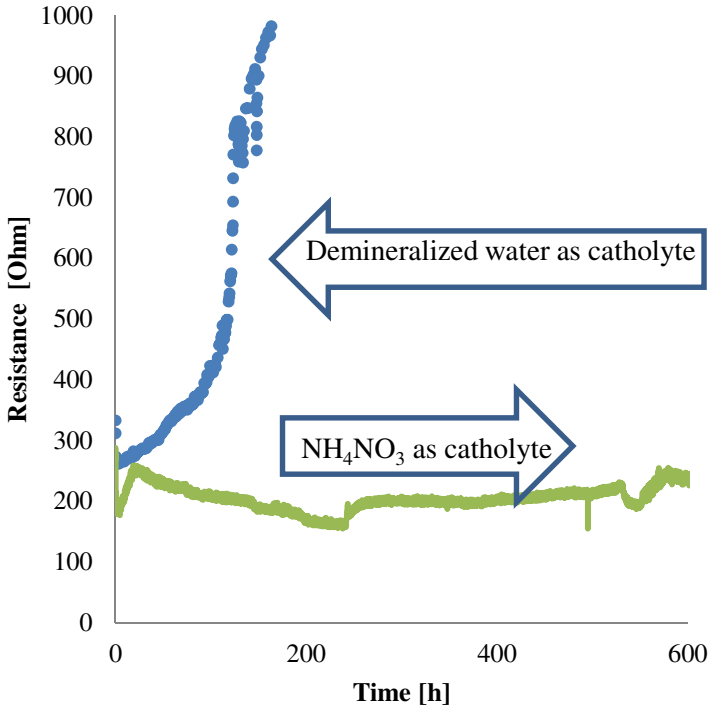

Figure 3-2. Ohmic resistance across the specimens with application of water or ammonium nitrate as catholyte solution

3.2.1.3 Specimen's sealing conditions

The curved surface of the specimen was sealed to enable leaching only in the longitudinal direction. A homogenized electrical gradient can be expected in the axial direction if the curved surface is completely sealed. Asphalt tape was utilized as the sealant material, and it also provided adequate elastic flexibility. As for dealing with high concentration gradients in the electrochemical cell, osmotic pressures might cause mechanical destructions, however, the application of an elastic sealant will prevent unrealistic degradation. Alternatively, silicon rubber can be utilized as an electrical-resisting sealing material. However, this product is rather expensive and not elastic enough.

The simulation of axial gradients, similar to the ones in natural leaching, was conducted in the electrochemical migration test by sealing only half of the curved surface of the specimen. Figure 3-3 and Figure 3-4 illustrate the changes in the simulated electrical gradient through the specimen when the sealing conditions were changed.

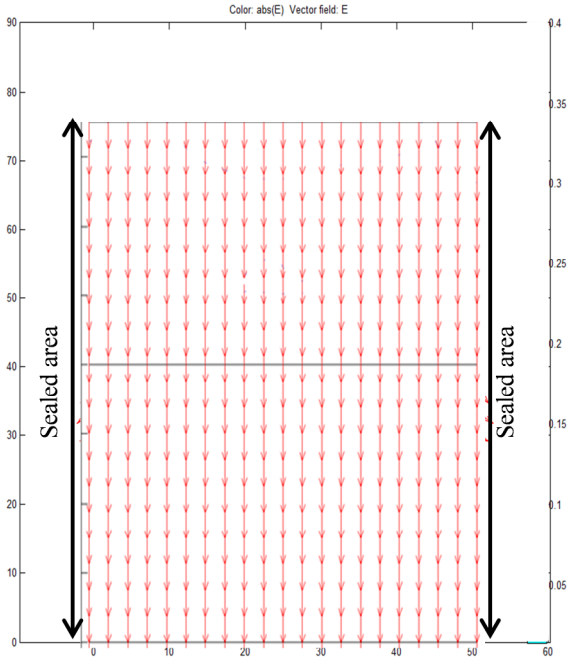

Figure 3-3. Electrical current inside the specimen sealing whole curved surface area of the specimen

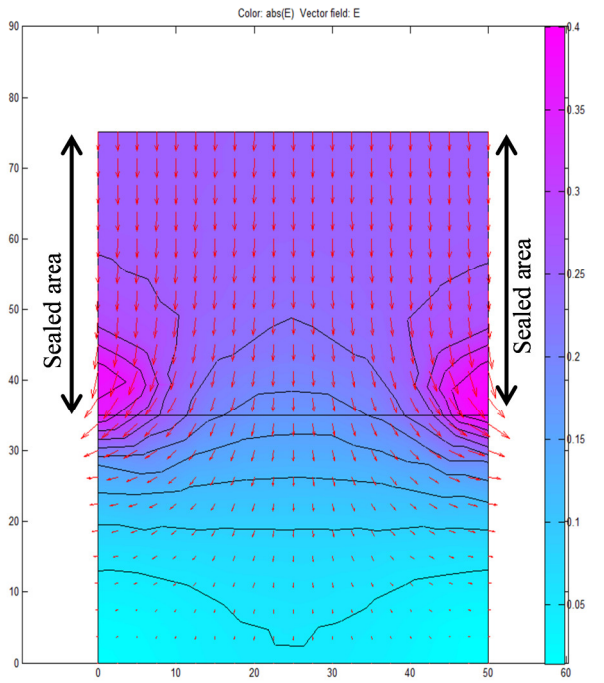

Figure 3-4. Electrical current inside the specimen sealing almost half of specimen's curved surface area

The results of such a test are presented in Paper I. Also the visual characteristics of the leached specimen when only half of the curved surface is sealed are presented in Figure 3-5. As can be seen in this figure, the changes in cross sections of the specimen are

illustrated as a function of time (the specimen was turned half way in to the experimental time to obtain a more homogenize leaching effect). As illustrated, leaching is not homogenized in the specimens due to the uneven distribution of electrical field.

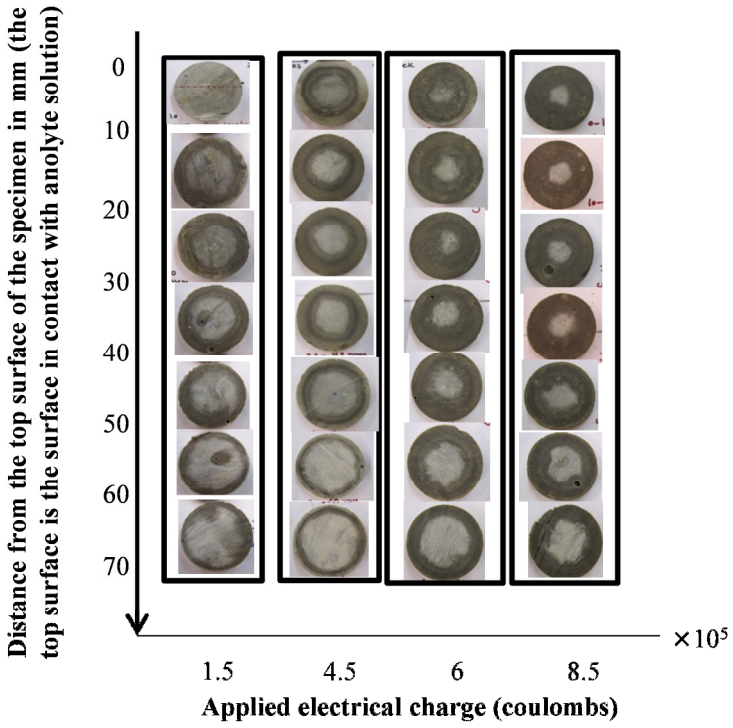

Figure 3-5. The observable changes inside the specimen in the course of the acceleration test

Considering these results, in order to completely control the leaching phenomenon in order to draw conclusions about the post-leaching characteristics of the specimens, a homogenized electrical gradient (sealing the whole curved surface) is recommended to be utilized in the final set-up design of the electrochemical migration method. It should be noted that, all of the results presented in this study (except the results in Paper I) are obtained using a completely sealed specimen.

3.2.1.4 Recharging reagents

In order to compensate for the consumed ions (OH^- and Li^+ ions from LiOH in the anolyte solution as well as H^+ and NO_3^- ions from ammonium nitrate in the catholyte solution), the solutions were frequently recharged. The quantities of the salts required for recharging were calculated according to Faraday's law of electrolysis as given in Equation (3.2).

$$I \cdot t = F \cdot z \cdot (\frac{m}{M}) \tag{3.2}$$

where, I is the current (A), t is the time (seconds), F is the Faraday number = 96485 C/mol, M is the molecular mass of substance (g/mol), m is the mass of substance (g) and z is the valance number of ions. Depending on the current intensity, different amounts of recharging reagents were used. The test method manual presented in Appendix also illustrates the calculation procedure to account for the needed regent amounts.

3.2.1.5 Specimen size

Cementitious specimens of sizes Ø50×75 and Ø100×50 mm were implemented in the electrochemical migration test. However, considering the homogeneous axial distribution of the electrical gradient utilized in this study, specimens of various sizes can be implemented. It should be noted that for specimens of different sizes, different magnitudes of current are needed to reach a similar current density. An important parameter to consider regarding mortar or concrete specimens is that only the paste fraction of the specimen is the current carrier (the ions only move in the pore solution of the paste). A detailed description of the calculation for the needed current necessary to reach the proposed current density is presented in Appendix. In the event of very high resistances due to a specific specimen size, lower current densities are recommended to prevent thermal cracking. If a lower current density is used, the required leaching time period must be extended to reach a given leaching state.

3.2.2 Experimental time

An important leaching level is considered to be the complete leaching of Portlandite as one of the major hydrated phases of HCP. Therefore, complete leaching of Portlandite which can also be calculated according to Portlandite content in the specimen (Table 3-2) was selected as the reference leaching level in this study. The accumulated leached calcium in the catholyte solution was frequently measured to account for the required experimental time to reach the leaching state of interest. As presented in Table 3-2, approximately 0.003 Moles of Portlandite exist in 1 gram of hydrated cement paste. As illustrated in Figure 3-6, with the application of a current density of 125-130 A/m^2, approximately 53 days of experimental time is needed to leach out this amount of Portlandite. However, lower current densities require longer leaching periods to obtain a similar leaching level. It should be noted that depending on the W/C-ratio the Portlandite content varies in the specimens. In this study the concrete specimens have the same volume of aggregate, implying the same

volume of CSH + Portlandite + capillary pores. Which means with a higher W/C- ratio, the capillary pore volume is larger, implying the CSH + Portlandite volume is smaller. Accordingly under the same degree of hydration, Portlandite in the concrete with higher W/C-ratio is less. As a consequence the experimental time for concrete specimens with W/C-ratio of 0.62 to reach to complete leaching of Portlandite should be shorter than that of specimens with W/C-ratio of 0.48. However, the prolongation of experimental time after leaching of Portlandite only affects the phase changes in CSH gel and as it was concluded by Carde et al. the changes in CSH phases due to leaching is not affecting the mechanical properties [36].

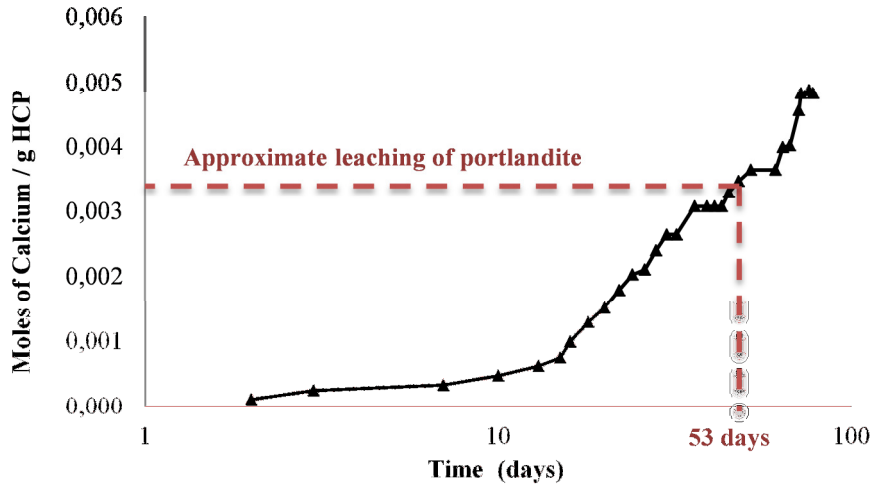

Figure 3-6. Leached calcium per gram of HCP against leaching time. The applied current density was 125-130 A/m^2.

3.2.3 Calcium migration rate

The transport or transference number is the fraction of the total current carried by given type of ions, Equation (3.3), where, I_+ is the current carried by a given type of ion, I is the total applied current, M is the number of moles of the given ions which are transferred, Z_+ is the valance number and t is the time. It should be noted that variations in the mobility and availability of the given ion in the system would cause different transport numbers.

$$t_+ = \frac{I_+}{I} = \frac{M \cdot Z_+ \cdot F}{I \cdot t} \tag{3.3}$$

Figure 3-7 illustrates the amount of leached calcium against the total applied electrical current for a specimen with the size of Ø50×75 mm. Considering 1 mole of leached calcium and 10^6 Coulombs of total applied electrical charge, the calculated transport number is 0.2 according to Equation (3.3).

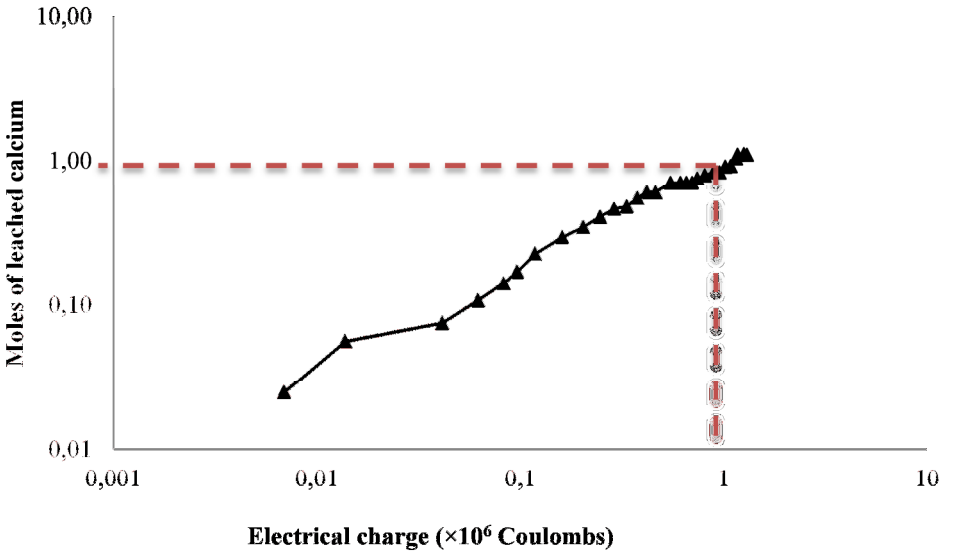

Figure 3-7. Moles of leached calcium against applied electrical current for a specimen with the size Ø50×75 mm.

Moreover, Figure 3-8 illustrates the changes in the rate of calcium leaching. The equivalent charge carried by leached calcium ions has been plotted against the total applied electrical charge per gram of cement paste. The tangent to the curve represents the transport number. As can be seen, the transport number is higher in Zone 1, it reduces for a short while and then increases again, while a gradual decrease can be seen in Zone 3. A plausible explanation for this behavior is that in the first few hours of the experiment the current was carried by the available calcium ions. However, after these ions have been transported with the applied current, additional dissolution of calcium-containing phases is needed. As ammonium nitrate was utilized in the catholyte solution, considering the migration of nitrates into the specimen, the considerably higher solubility of calcium nitrate will cause an increase in the ionic concentration of calcium in the pore solution (Zone 3), thus the migration of calcium will propagate. As the leaching propagates, the available concentration of the calcium ions decreases as well, which leads to a gradual decrease in the transport number of these ions in Zone 3.

It should be noted that the transport number of calcium ions (slope of the curve in Figure 3-8), in Zone 1 and 2 is obtained only based on 2 measured points. This might cause some uncertainty in absolute values for the transport number. However, the decrease in rate of calcium migration in Zone 2 and the following increase in the rate in Zone 3 was shown to be repeatable in comparable sets of experiments.

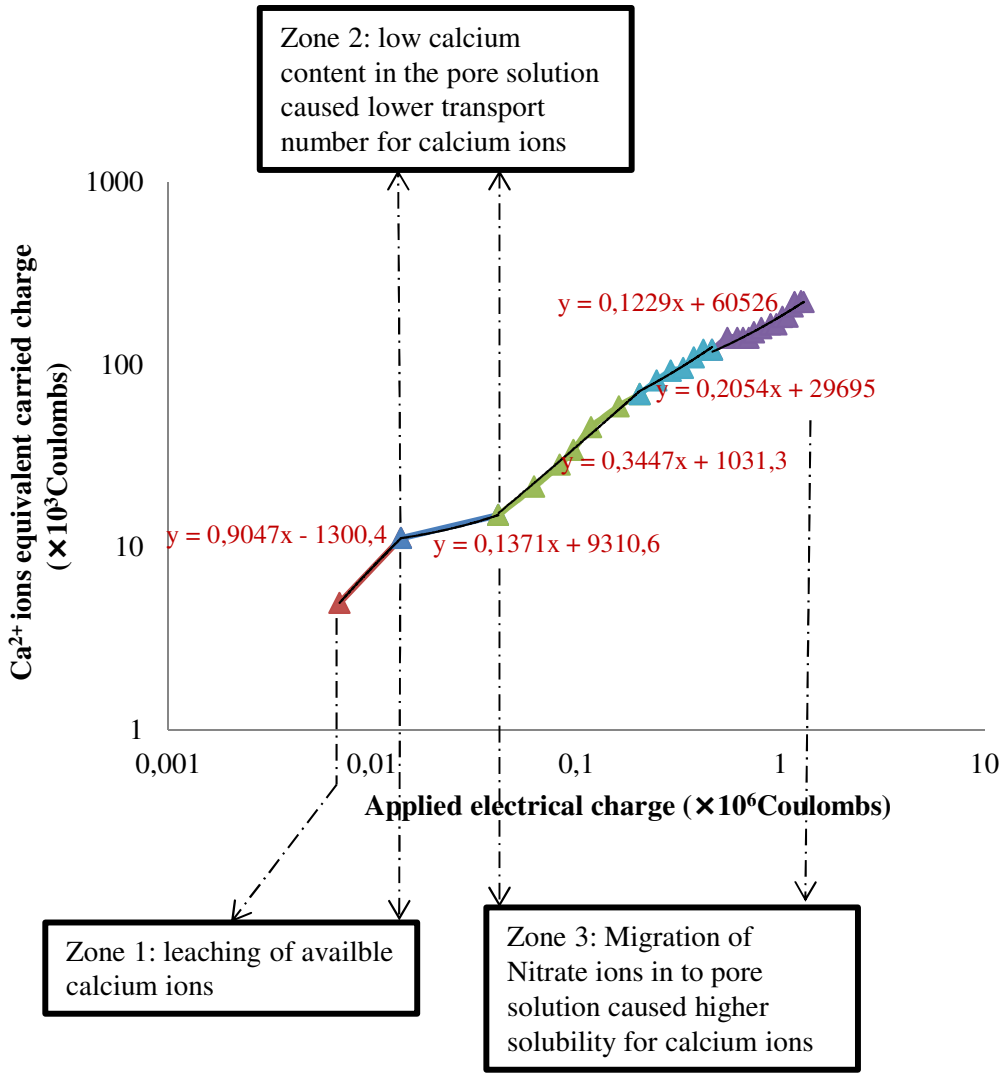

Figure 3-8. Frequent changes in the rate of calcium migration represent the changes in the calcium transport number

3.3 Characterization methods

Several instrumental analyses as well as experimental investigations of properties were carried out to account for the changes in chemical, mineralogical, physical, mechanical and

transport properties of the aged specimens. The experimental details of the laboratory analysis are explained in this section.

3.3.1 Chemical and mineralogical analysis

3.3.1.1 IC and potentiometric titration

To quantify the content of charged substances in the catholyte solution, Ion Chromatography (IC) was utilized using an IONEX (ICS 900) Ion Chromatograph. IC allows the ions of interest to be detected through conductivity or UV/visible light absorbance. The samples were injected into the instrument with an auto-sampler. In addition, the gradual change in the calcium concentration in the catholyte solution was analyzed with potentiometric titration on a Metrohm Titrator 702 SM Titrino, using a calcium-selective electrode and a 0.1 N EDTA solution as the titrant.

3.3.1.2 XRD

Characterization of the crystalline phases in the solid samples was performed with X-Ray Diffraction (XRD). A Siemens D5000 (CuKα = 1.5418 Å) X-Ray diffractometer equipped with a Gobel mirror was used. The measurements were carried out by using 0.050˚ per step and at a time step of 2 s. Powder sample was prepared by crushing and grinding the solid sample in a mortar while immersed in ethanol, and vacuum dried after grinding. For each analysis, 0.5 grams of the powder placed on a thin-walled glass sample holder was used. The results were calibrated using 0.05 wt.% of Si powder as the internal standard.

3.3.1.3 LA-ICP-MS

Line scans quantifying the axial (longitudinal) changes in Ca/Si ratios of solid samples were performed using Laser Ablation-Inductive Coupled Plasma-Mass Spectrometry (LA-ICP-MS). Laser Ablation analysis was performed using a New Wave NWR213 instrument coupled to an Agilent 7500a quadrupole ICP-MS (upgraded with a shield torch and a second rotary vacuum pump). A 30-micron laser spot size, with a beam energy density of 6 J/cm^2 and a repetition rate of 10 Hz was used in line scan mode (scan speed 100 µm/sec). Each analysis included background measurements for 30 seconds, before switching on the laser.

3.3.1.4 SEM/EDX

The surface topography and elemental composition of the solid samples were analyzed with Scanning Electron Microscopy (SEM). A FEI Quanta ESEM 200 equipped with a field emission gun and an Oxford Inca EDX system was used to perform the analysis. Thin cubes of the solid sample of about 20×10 mm with a thickness of 10 mm were used. The samples were vacuum dried prior to analysis. It should be noted that in order to prevent the samples from carbonation they were neither polished nor coated which may cause charging effects in the results as well as uncertainties due to the uneven surface of the sample. The EDX (Energy Dispersive X-ray) analysis were performed in high vacuum mode and at a working distance of 12 mm.

3.3.1.5 XRF

X-Ray Fluorescence (XRF) analysis were performed to quantify the elemental composition of the samples. The analysis were carried out using an X-ray Fluorescence sequential spectrometer (PANalytical, AXIOS) by dispersion of wavelength (WDXRF) with a Rh tube and three detectors.

3.3.1.6 TGA/DSC

Thermogravimetric (TGA) and Differential Scanning Calorimetric (DSC) analysis indicate the changes in mass and heat of reaction as a function of temperature. Unalike TGA/DSC spectrums represent different materials. Consequently changes in hydrated phases of cementious materials, specifically Portlandite can be detected. The analysis were performed with a Netzsch STA 409 PC/PG. The samples were placed in a crucible and heated in pure nitrogen (inlet flow rate of 20 ml/min) to a set temperature of 900°C. The heating rate was a linear ramp of 10°C/min.

3.3.1.7 NMR analysis

Nuclear Magnetic Resonance spectroscopy (NMR) was used in this study to assess the changes in physical and chemical properties of atoms or the molecules in which they are contained and to obtain information about the structure of molecules. This technique exploits the magnetic properties of certain atomic nuclei with respect to nuclear magnetic resonance. Changes in the structure of silicates were considered which represents changes in the structure of CSH gel. NMR spectroscopies in this study were performed on a Varian

Inova-600 operating at 14.7 T and equipped with a 3.2 mm solid-state probe. Measurements were conducted at 299 K with a MAS spinning rate of 15 kHz.

3.3.2 Analysis of physical properties

3.3.2.1 Pore structure and specific surface area

The pore size distribution was studied with Mercury Intrusion Porosimetry (MIP), using Micrometrics Auto pore 9500 with a 5 ml penetrometer. In this method, the volume intrusion of mercury into specimen pores is measured to determine pore size distribution. The relation between pore sizes and the applied pressure is presented in Equation (3.4):

$$p = \frac{2\gamma \cos\theta}{r} \tag{3.4}$$

where p is the absolute applied pressure, γ is the mercury surface tension, θ is the contact angle and r is the pore radius. It should be noted that in this method the pores are assumed to be cylindrical. Moreover, the Brunauer-Emmett-Teller (BET) specific surface area and Barrett-Joyner-Halenda (BJH) pore size distribution was measured with N_2 adsorption with a Micrometrics TriStar 3000. BET analysis provides specific surface area assessments of materials by nitrogen multi-layer adsorption which is measured as a function of relative pressure. The technique encompasses external area and pore area evaluations to determine the total specific surface area in m^2/g. Also, by employing BJH analysis, pore size distribution, independent of external area due to particle size of the sample can be characterized.

3.3.2.2 Freezable water

The changes in freeze-thaw regimes due to decalcification, were accounted for with scanning colorimetric measurements. A Calvet-type scanning calorimeter (SETARAM) was used. The calorimeter was calibrated and operated to work between about 20 °C and about -130 °C. The temperature scanning of a freezing and melting cycle started at 20 °C and went down to -80 °C and then went back to 20 °C again. The cooling and heating rate were set to be 0.1 °C per minute. The cement paste/mortar samples were dried at +50 °C and then vacuum saturated. The visible water on the surface of cylinders was wiped off and the samples were assumed to be saturated surface dry when placed in the calorimeter. The mass of each vacuum saturated sample was determined before and after calorimetric

measurements. The mass difference was less than about 0.1%. After calorimetric measurements, the samples were subjected to oven drying at 105 °C until constant dry weights could be determined.

3.3.3 Assessment of transport properties

3.3.3.1 Diffusion cell tests

Conventionally, the diffusivity of ions in a porous material is measured using a natural diffusion cell test at a certain gradient of concentration [16]. In the set-up of the natural diffusion cell test, as presented in Figure 3-9 two solution containers (cells) were separated by a 10 mm thick slice of a paste specimen. The cell filled with a solution containing the specific ions of interest is called the upstream solution and the other cell, which is free of those ions (usually filled with deionized water), is called the downstream cell. The diffusion of the ions of interest would take place from the upstream cell to the downstream cell, through the specimen, due to the concentration gradient between the cells. In order to study the effect of ionic charge and solution concentration on the transport properties of chloride, sodium, lithium and calcium ions, 6 different solutions containing these ions were used:

- 5 g, 10 g and 20 g NaCl per liter
- 10 and 20 g LiCl per liter
- 10 g $LiNO_3$ per liter

In this study, 18 sets of diffusion cells were used, with three sets per each solution. Monitoring the concentration changes in the downstream cell, and using Flick's first law, the steady state diffusion coefficient can be calculated according to Equation (3.5) [81].

$$D_{steady-state} = \frac{V \cdot \Delta Q}{A \cdot \Delta t} \times \frac{L}{(C_1 - C_2)} \tag{3.5}$$

where V is the volume of the downstream cell (m^3), ΔQ is the increase in the specific ions in the downstream cell (kg/m^3), Δt is the time interval (s), A is the exposed specimen surface area (m^2), L is the exposed slice thickness (m), C_1 is the concentration of the

specific ions in the upstream solution (kg/m^3) and C_2 is the average concentration of the specific ions in the upstream solution (kg/m^3).

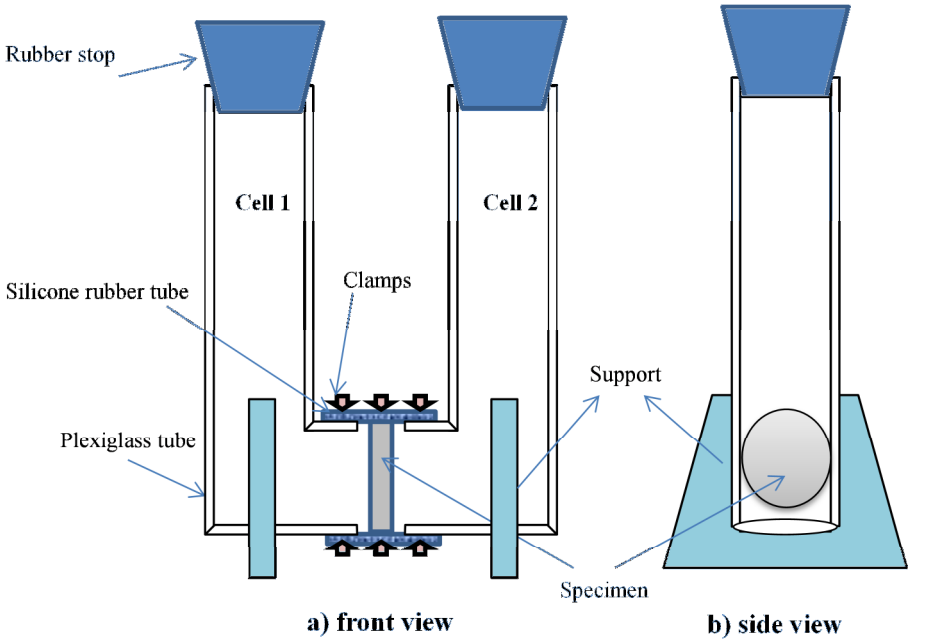

Figure 3-9. Diffusion cell test set-up design: front view (a) and side view (b)

Using the Q_{Cl}–t curve the "time-lag", which is the duration until a significant linear relationship is observed from the Q_{Cl}–t curve could be specified. The non-steady state diffusion coefficient was calculated using Equation (3.6) [81]:

$$D_{non-steady-state} = \frac{L^2}{6 \times t_n} \tag{3.6}$$

where L is the thickness of the specimen (m) and t is the time-lag (s).

3.3.3.2 Diffusion-Adsorption test

In order to compare the diffusion properties of reference and calcium-depleted specimens, the diffusion cell test was performed by utilizing solutions of LiCl, NaCl and CsCl with 2 different concentrations of 0.05 and 0.5 M. Moreover, to analyze the changes in adsorption properties, the reference and the calcium-leached paste specimens were hand crushed and powdered in a mortar and mixed with a CsCl solution in separate plastic tubes in a glove

box filled with nitrogen gas in order to prevent the samples from carbonation. The Cs concentration in the solutions was determined with ion chromatography.

3.3.3.3 Gas permeability and capillary water absorption

The gas permeability and capillary water absorption tests were performed according to the state of the art report of RILEM Technical Committee 189-NEC [82] and the recommendations by Kollek [83]. The measurements were performed on concrete specimens of Ø100×50 mm. The specimens were preconditioned for two weeks according to the recommended procedures stated in the RILEM technical report 189-NEC [82] and the recommendations by Kollek [83] prior to the measurements. Two specimens, representative for each W/C-ratio and each degradation state, were tested to ensure repeatability of the results.

3.3.4 Measurement of mechanical properties

3.3.4.1 Tensile and compressive strength

The tensile strength of the leached and reference concrete specimens of Ø100×50 mm was measured using the splitting test on a Toni-Technik compression testing machine with a maximum capacity of 100 kN. The test procedure was in accordance with the American standard ASTM C49 [84]. The compressive strength of concrete, mortar and paste specimens of Ø50×75 mm was measured with the same compression testing machine and according to the ASTM C39 standard [85].

3.3.4.2 Elastic modulus

The elastic modulus of the concrete specimens of Ø50×75 mm was obtained as the slope of stress-strain curves recorded by means of an ALPHA compression testing machine, Figure 3-10. The load cell had a maximum capacity of 50 kN and was loaded with a mechanical press. The vertical strain was measured using a calibrated Linear Variable Differential Transformers (LVDT) sensor. The end surfaces of each specimen, perpendicular to the longitudinal axis of the specimen, were cut with a diamond saw and polished in order to create a smooth surface. Concrete specimens of Ø50×75 mm were placed between two platens and positioned under the load cells. 4 LVDT sensors were used to measure the displacement of the bottom platen and three more sensors were employed to measure the displacement of the upper platen. The sensors were connected to a data-log system to

record the gradient of strain as a function of stress. The calcium-depleted specimens were kept in 100% RH prior to test in order to avoid any drying cracks.

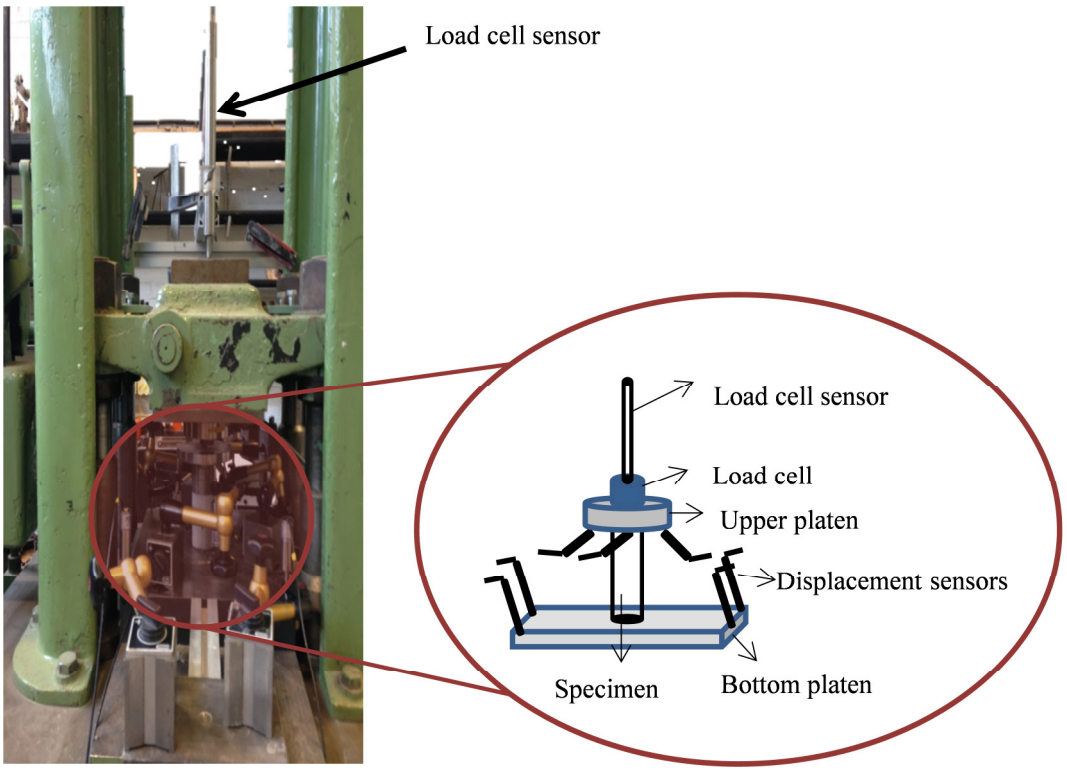

Figure 3-10. Elastic modulus measurements set-up design

3.3.4.3 Resonant frequency test (fundamental longitudinal frequency)

An impact resonant apparatus was used to measure the fundamental longitudinal frequency of concrete, mortar and paste specimens of Ø50×75 mm. One end of the horizontally placed concrete cylinder was vibrated with an impactor, and the other end was connected to an accelerometer. The accelerometer was connected to an amplifier, and the set-up was connected to a wave-form analyzer. The wave-form analyzer should have a sampling rate of at least 20 kHz and should record at least 1024 points of the wave form. By utilizing the fact that the elastic modulus is proportional to the square root of the resonant frequency, the elastic modulus of each specimen can be calculated according to the American standard ASTM C215 [86].

3.4 Reference leaching test methods

Several leaching tests designed according to methods proposed in the literature were carried out in the pilot scale of this project. The outcomes demonstrate the comparability of the produced aged samples with the specimens manufactured with application of the electrochemical migration method. Since the rate of leaching would increase when using cementious samples with reduced particle size, most of the tests were performed with powder samples.

3.4.1 Natural immersion test

The natural immersion test involved immersion of the test specimen in a solution containing the specific ions of interest and measuring the penetration or leaching depth or profile of these ions in the specimen. In this test, a total of 20 cylinders (10 pastes and 10 mortars) of Ø46×100-250 mm, cured for 6 months, were coated with thick (3-4 mm) epoxy, sealing all surfaces except one for exposure. The specimens were immersed in ground water 400 meters deep under the ground in the Äspö laboratory located in Oskarshamn, Sweden, Figure 3-11. After 2 and 3.5 years of exposure, samples were chemically analyzed in order to obtain their leaching profiles.

Figure 3-11. Natural immersion test

3.4.2 Flash column test

The flash column test was designed considering the effect of an advective flow and reduced particle size on leaching. The set-up design as illustrated in Figure 3-12, includes a 110 ml

glass chromatography column with a fritted disc equipped with a PTFE plug to control the flow rate. A powder sample of about 0.1 mm (0.075-0.125) was filled into the column on the fritted disc and subjected to upward water flow with a flow rate of less than 2.5 ml/s. The column was connected to a reservoir with the capacity of 5 liters through PVC tubes from both sides. Demineralized water was used as the circulating solution in the system. The pH value of the solution was manually monitored. When the pH value in the circulating solution was around 12, the entire solution in the reservoir was refreshed. The experiment was continued until the pH value in the solution became constantly low (about 8). A similar set-up design can be found in a study presented by Pfingsten and Shiotsuki [15].

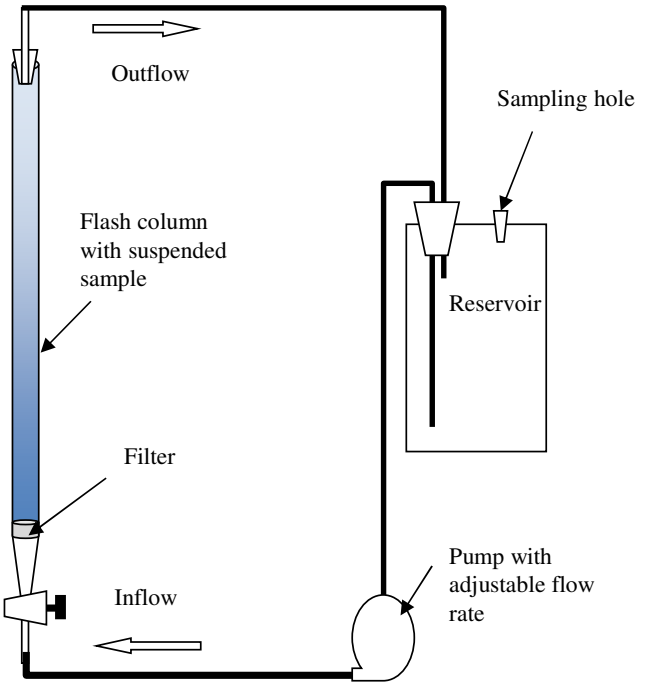

Figure 3-12. Flash column test set-up design

3.4.3 pH stat test

The pH stat test was designed enabling accelerated leaching of calcium which was obtained as of using reduced particle size and lower pH level [7] of the leaching solution than that of in pore solution. In this method, a constant pH level lower than that of the natural situation was applied to powdered samples through frequent acidification. The added volume of acid and the changes in temperature for an experiment aiming for pH=8, is presented in Figure 3-13. A powder size of about 0.1 mm (0.075-0.125) was used in this test. In order to prepare the powder, thin slices were cut from a cylindrical specimen after more than 6

months of moist curing. The slices were crushed and ground under wet conditions in order to reduce the risk of carbonation. 12 grams of the produced powder was mixed with 50 ml of Milli-Q water and 6.5 ml of concentrated Nitric acid (67% chemical quality) which was added to the mix to reach the initial pH of 8.

The automated potentiometric titration method using a Metrohm 836 Titrando titrator was employed to perform the test. The titrator was equipped with a magnetic stirrer as well as two dosimeters. The pH electrode with a built in thermometer was used to monitor the pH value in the solution. The electrode was calibrated with standard buffer solutions before use. The titration procedure was controlled with TIAMO software. Nitric acid of 3.7 M was used to maintain the natural pH value of 8. The experiment duration was set to 24 hours because stable equilibrium was observed under this time period. After termination of the experiment, the solid part was separated from the liquid through vacuum filtration. The sample was vacuum dried to be further characterized.

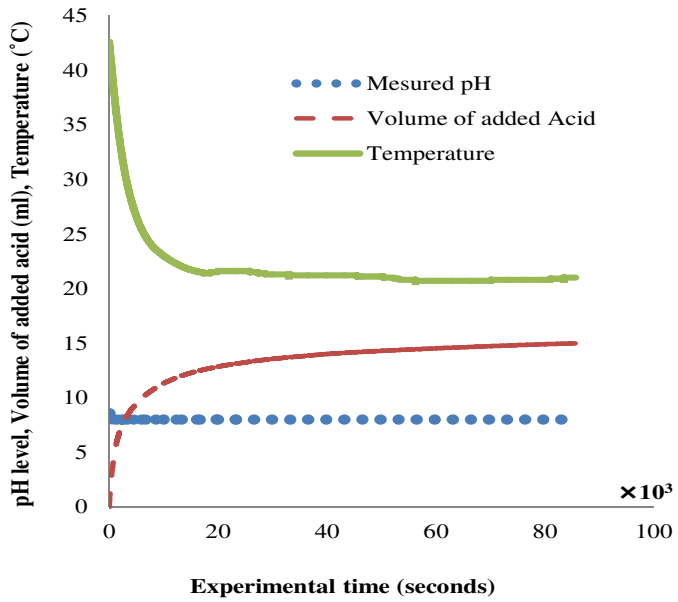

Figure 3-13. Temperature change and the added amount of acid as a of function of time in pH stat test for pH level 8.

3.4.4 Application of concentrated ammonium nitrate solution

It was mentioned in Chapter 2 that one of the leading chemical acceleration methods in the literature is the application of concentrated ammonium nitrate solution [26, 37]. It was noted that to obtain a high acceleration rate specimens of small sizes were used which

limited further proper testing of properties. However, it can be informative to repeat this method and compare the properties of the aged samples with the samples aged with other leaching methods as well as the electrochemical migration method.

As shown in Figure 3-14, thin cylinders (Ø10 mm) of paste samples cured for 1 year were immersed in 6M ammonium nitrate solution in a vacuumed desiccator container (the container was vacuumed to prevent carbonation). The content was stirred during the experimental time (using a magnetic stirrer) to homogenize the effects. The experimental time was set to 45 days, in line with the results reported by Heukamp et al. [26].

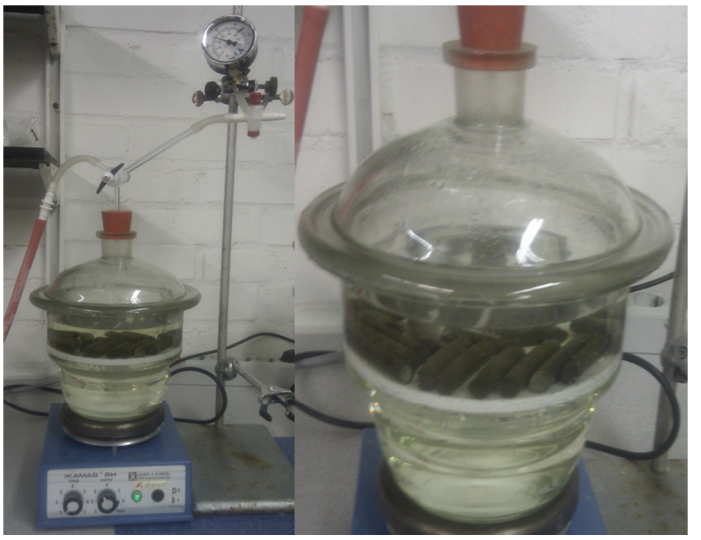

Figure 3-14. Accelerated leaching test with application of concentrated ammonium nitrate solution

4 Results and Discussions

The outcomes of this project are presented in the following. The results are categorized with regard to the major goal of this study which is to study the various properties of decalcified cementitious materials. It was noted in the previous chapter that in order to reach this goal an important part of the study was to develop a test method to produce decalcified cementitious specimens of flexible size.

The set-up design of the method was presented in the previous chapter and it was noted that the method is applicable for samples of variable size. The efficiency of the method in calcium migration was demonstrated and the novelty of the method accelerating both dissolution and diffusion processes involved in decalcification of cementitious materials was discussed. In this chapter, the results of through characterization of leached specimens with respect to instrumental analysis results are presented. Also, the changes in chemical, mineralogical, physical, transport and mechanical properties of calcium leached specimens produced with application of electrochemical migration method are discussed. The characteristics of decalcified specimens produced with application of the electrochemical migration method and the reference methods, are compared. The comparability of the leached specimens is an indication of credibility of the electrochemical migration method. Specifically the similarity with natural immersion test is of high importance. However, it should be mentioned that detailed characterization of specimens leached with reference accelerated leaching test methods is out of the scope of this study. As it was noted in Chapter 2, these methods do not enable the leaching of specimens of flexible size and consequently are not comparable with electrochemical migration method in this regard.

The chemical and physical characterization results can be found in Paper II and partially in in Paper IV, V and VI. The results regarding changes in mechanical properties are presented in Paper IV, V and VI. The changes in transport properties are presented in paper VI and partially III and IV. Discussions regarding characteristics of specimens degraded with natural immersion can be found in Paper V and VI.

4.1 Chemical and mineralogical properties of leached specimens

The LA-ICP-MS results, presenting the electrochemical migration induced longitudinal changes in the Ca/Si-ratio of paste specimens as a function of leaching duration are illustrated in Figure 4-1. As can be seen, the reference specimen had a relatively homogeneous distribution of Ca/Si-ratio, which decreased with the propagation of the leaching front from the cathodic side towards the anodic side. The longitudinal function of changes in the Ca/Si-ratio propagated towards a relatively homogeneous leaching state in time, which is the complete leaching of Portlandite. It should be noted that leaching of Portlandite is also accompanied by phase changes in CSH gel.

The reference lines presenting the Ca/Si-ratio of the Portlandite leaching state as well as the Ca/Si-ratio of CSH were calculated according to Table 3-2, as shown in the previous chapter. As can be seen, after approximately 53 days of experimental time (1×10^6 Coulombs), a Ca/Si-ratio close to complete leaching of Portlandite was obtained. As mentioned in the previous chapter, 53 days of leaching is the proposed experimental time for the electrochemical migration method. This means that in upcoming results and discussions, the leaching state representing degraded specimens by utilizing the electrochemical migration method corresponds to approximate leaching of Portlandite. In addition, based on XRF analysis, the longitudinal changes in the Ca/Si-ratio of the degraded specimen leached for 53 days are presented in Table 4-1. The results are relatively comparable with the results from the ICP-MS analysis as shown in Figure 4-1. The results also indicate that a depletion depth of 75 mm can be expected with the application of the electrochemical migration method after 53 days of experimental time. Considering the leaching experiments reported in the literature, Haga [27] have shown that a depletion depth of maximum of 1.25 mm can be expected after 100 days of a natural immersion test. In a similar experimental approach, Faucon [31] have shown that up to 60 days of natural leaching leads to 0.7 mm of dissolved thickness in exposed specimens. Also according to investigations by Trägårdh and Lagerblad [9, 23] a leaching depth equal to 5-10 mm can be expected after up to 100 years. Moreover, considering the results presented by Carde and Francois [37], with the application of concentrated ammonium nitrate solution a degraded thickness of 8 mm can be expected after 36 days of leaching. Comparing these results with the depletion depths of 75 mm for the specimens leached with

the electrochemical migration method presented in this study, it is stablished that a considerable acceleration rate can be obtained using the electrochemical migration method.

The changes in the Ca/Si-ratio indicate possible changes in the calcium-containing phases in HCP. XRD analysis results presented in Figure 4-2, illustrate the crystallographic changes caused by leaching. As can be seen, the most apparent change is that the Portlandite peaks had disappeared in leached samples.

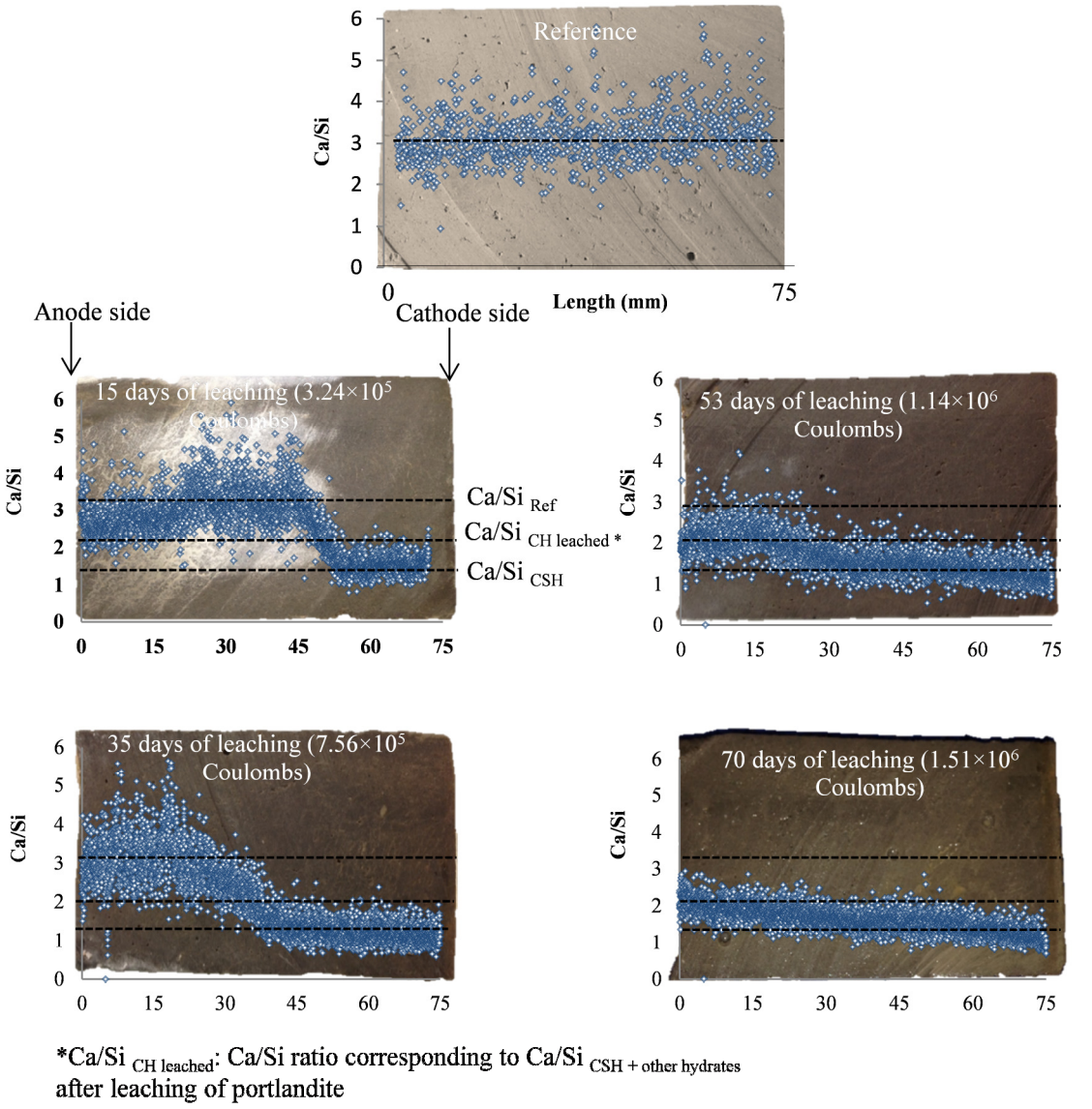

Figure 4-1. Longitudinal LA-ICP-MS results (considering 250 mA of constant current for a paste specimen of Ø50×75 mm)

Table 4-1. XRF analysis results (The aged paste sample had been leached for 53 days.)

	% weight	SiO_2	Al_2O_3	Fe_2O_3	MnO	MgO	CaO	K_2O	SO_3	Ca/Si
	Reference	16.8	2.8	3.6	0.2	0.6	49.5	0.5	1.1	3
Aged sample (Distance from anodic side)	**0-15**	17.2	2.9	3.6	0.2	0.6	37.4	0.0	0.9	2.2
	15-30	19.2	3.3	4.0	0.2	0.6	40.6	0.0	0.6	2.1
	30-45	20.9	3.5	4.3	0.2	0.8	36.9	0.0	1.2	1.8
	45-60	21.4	3.7	4.4	0.3	0.7	33.6	0.0	0.6	1.6
	60-75	20.2	3.4	4.2	0.2	0.8	27.2	0.0	0.8	1.4

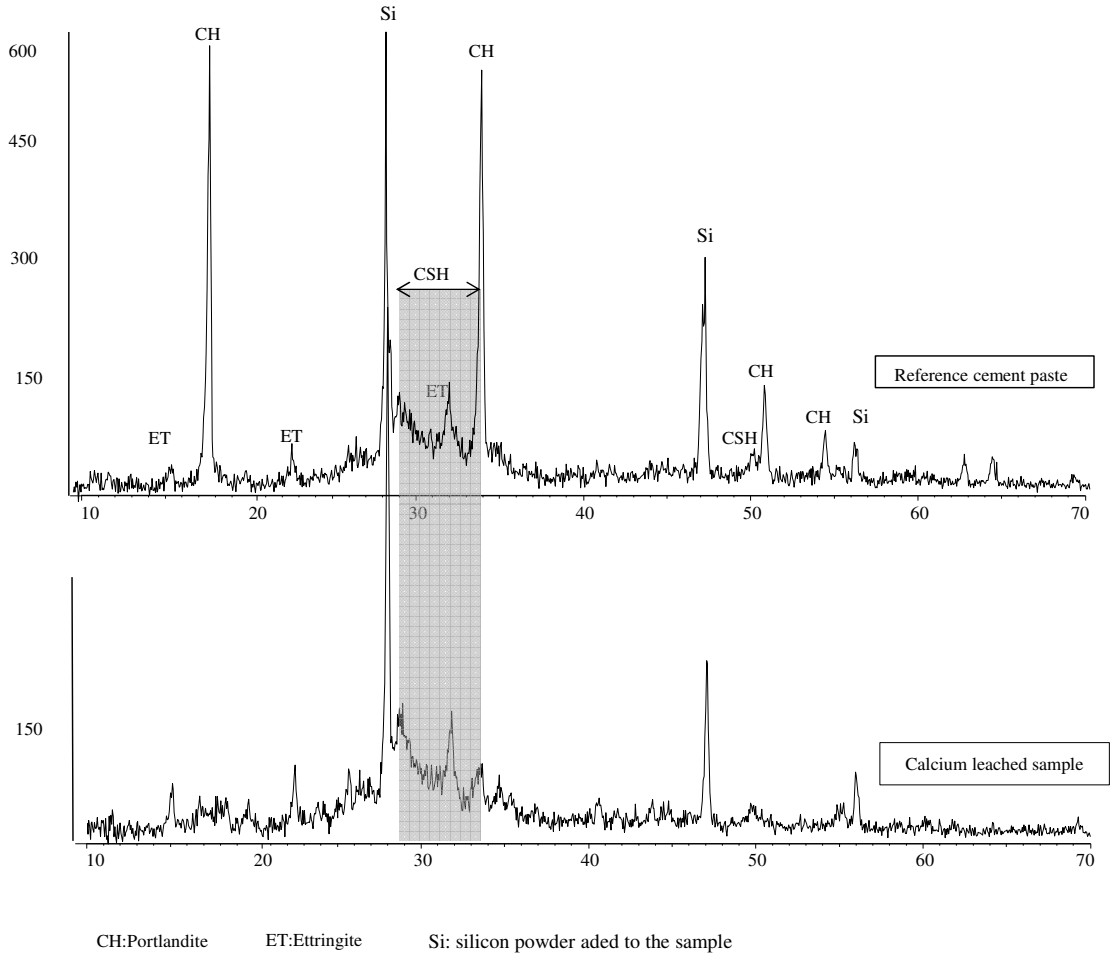

Figure 4-2. XRD analysis results comparing the un-leached reference and the leached sample. (The aged paste sample had been leached for 53 days.)

To account for the credibility of XRD results, TGA analysis were conducted and the results are shown in Figure 4-3. As can be seen, the reference sample exhibits a mass change at approximately 400°C, which is the assigned peak to Portlandite [87]. However, thermogravimetric changes in the leached sample do not show any Portlandite peak. The preferential leaching of Portlandite, as stated in Chapter 2, has also been reported in the available leaching assessments in the literature [27, 42, 88].

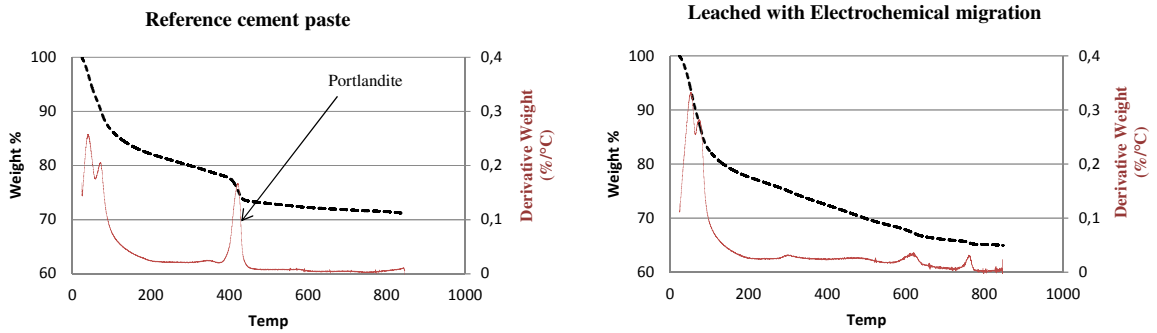

Figure 4-3. TGA analysis comparing changes in temperature-induced mass changes in cement paste samples due to leaching. (The aged paste sample had been leached for 53 days.)

In addition, Figure 4-4 illustrates comparable thermogravimetric outcomes for leached mortar and concrete samples. This indicates that leaching of Portlandite with the application of the electrochemical migration method was not affected by the addition of aggregates in the cementitious specimens.

4.2 Physical properties of leached specimens

4.2.1 Pore structure and specific surface area

The visual changes in the pore structure of leached paste specimens are illustrated in Figure 4-5. It can clearly be seen that the degraded samples are considerably more porous than the reference samples. Moreover, the Portlandite crystals can be found in the reference samples while crystalline phases cannot be seen in the images representing leached samples.

A more detailed assessment of the changes in pore structure and the distribution of pore sizes are presented in Figure 4-6 with regard to mercury intrusion and N_2 adsorption analysis. As can be seen, the mercury intrusion results indicate changes in the larger pores (capillary pores) and the N_2 adsorption results show changes even in gel pores. The results indicate a considerable increase in pore volume due to leaching. As shown, a major

increase in capillary pores happens for pores of size approximately 200 nm. This has also been shown by Haga (2005).

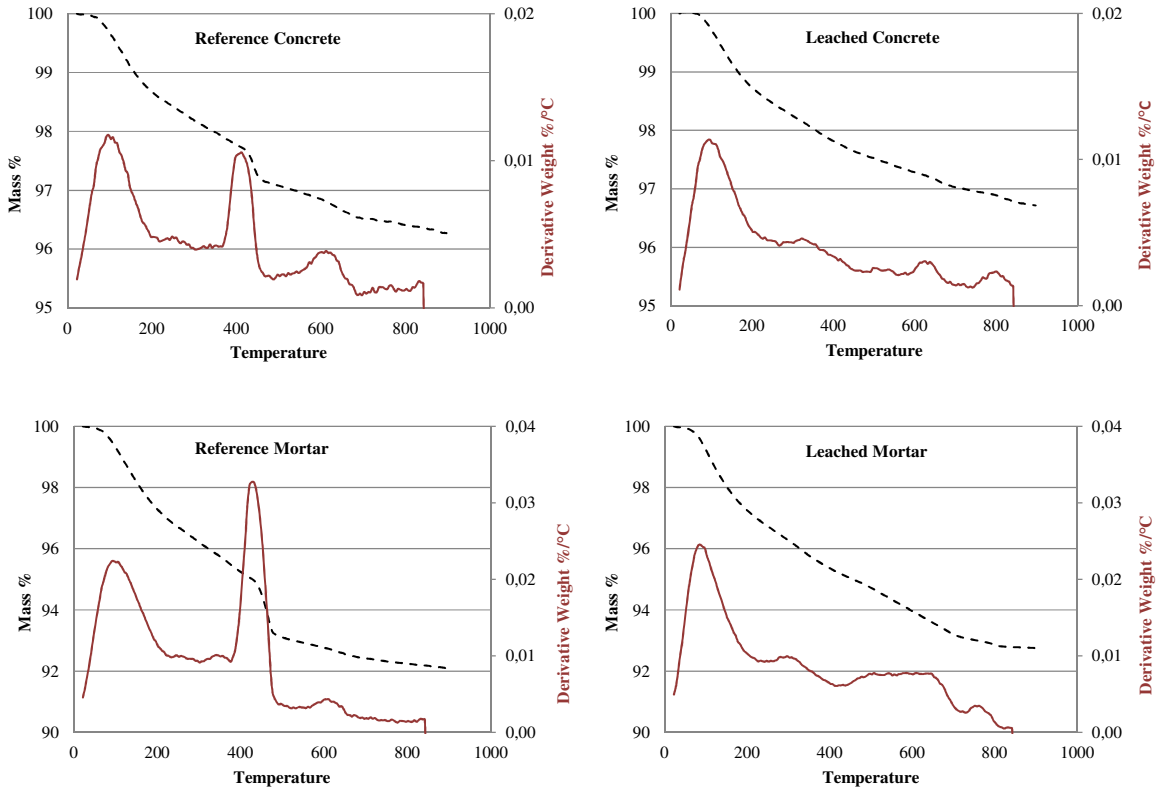

Figure 4-4. TGA analysis comparing changes in temperature-induced mass changes in concrete and mortar samples due to leaching. (The aged samples had been leached for 53 days.)

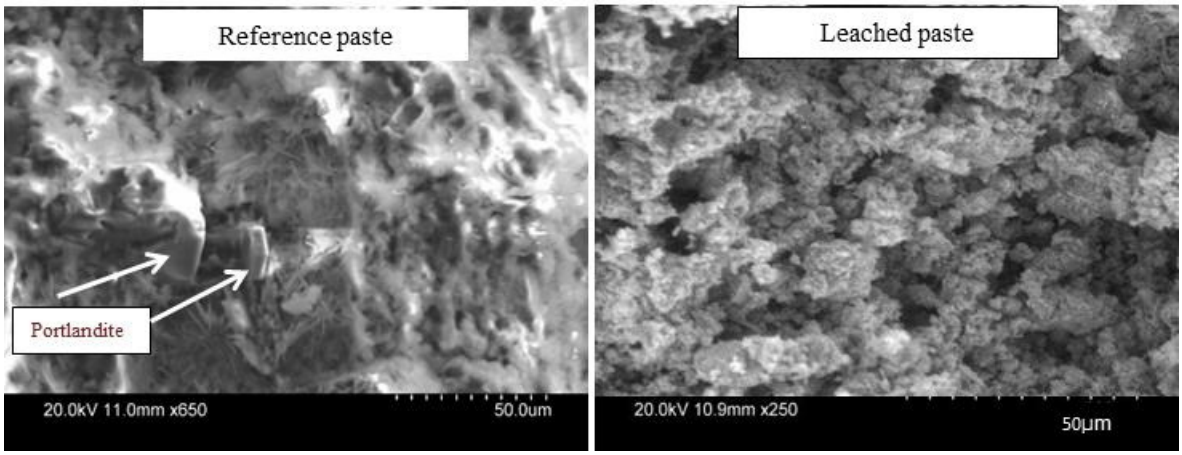

Figure 4-5. SEM images from reference and leached paste samples. (The aged paste sample had been leached for 53 days.)

Another important point is the 50 nm pores. The results reported by Haga (2005) indicate a lower pore volume in this pore size for the leached sample than in the reference material. However, Figure 4-6 indicates relatively similar pore volume for this pore size before and after aging with electrochemical migration method. The results presented in Figure 4-7 can clarify this difference. The figure shows that the pore volume assigned to this pore size in the samples leached for 25 or 35 days is actually lower than the reference, which is comparable to the results presented by Haga (2005). since a decrease in pore volume can be due to precipitation, the results indicate that the probable leaching-induced precipitations also occur when using the electrochemical migration method, however, with longer leaching time these precipitations are also leached out.

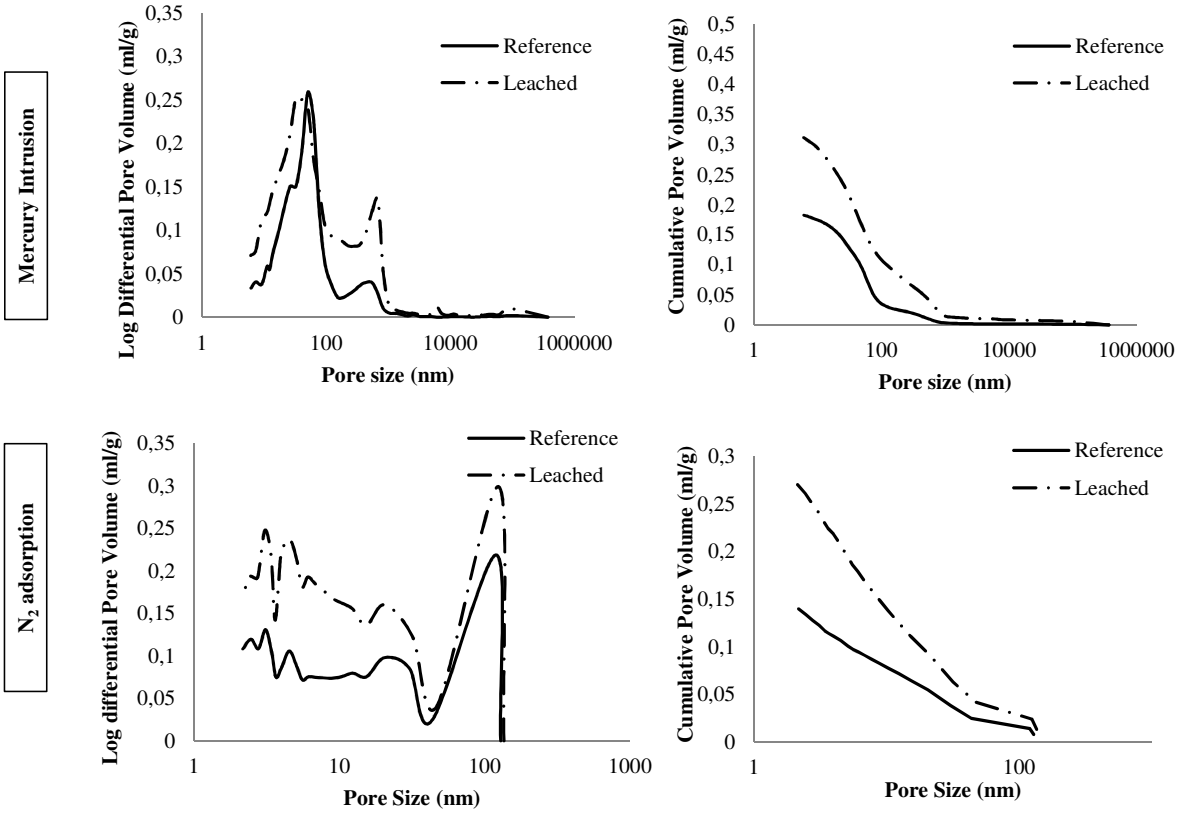

Figure 4-6. Pore size distribution results: mercury intrusion and N_2 adsorption analysis. (The aged paste sample had been leached for 53 days.)

Moreover, the N_2 adsorption results, Figure 4-6, indicate a considerable increase in gel pores. Although the contribution of the changes in pore volume of the gel pores is considered to be negligible in total pore volume increase [27, 36], a greater gel pore volume

indicates changes in other parameters such as specific surface area. BET analysis results indicate that leaching causes an increase of approximately 80% in specific surface area of cementitious materials. This is in agreement with the results presented by Chen et al. [89] indicating that a near doubling of specific surface area is expected due to decalcification of cementitious materials with changes in Ca/Si-ratio from 3 down to 1.1. It should be noted that the deviations in measured specific surface area by BET is a known disturbing phenomena as reported in literature [51], specifically due to the effect of the drying condition of sample prior to the analysis. However, this matter should not influence the conclusions in this study as all sets of measurements were carried out under the same conditions and showed similar specific surface areas for degraded specimens with both electrochemical and natural leaching methods with values higher than that of reference sample.

A plausible explanation for the increase in specific surface area is the changes in characteristics of the scale of gel pores due to silicate polymerizations in the CSH gel. It has been reported in the literature that due to leaching, the Ca/Si-ratio of CSH gel gradually decreases and iron or aluminum ions dissolved from Ettringite and AF_m phases can incorporate into the CSH [30, 31, 42, 88]. As also stated in Chapter 2, a higher specific surface area in the CSH gel indicates the presence of available adsorption sites for other ions, such as aluminum and iron.

The NMR results are presented in Figure 4-8 illustrating the changes in the structure of ^{29}Si, thus representing the changes in the structure of CSH gel. As shown Q_2 peaks are increasing due to leaching. This indicates a higher degree of polymerization of silicates as Q_2 represents a longer chain structure. The Q_1 and Q_2 peaks are located according to a study by Rawal et al. [90]. Silicate polymerization as a phenomenon caused by decalcification has been reported in literature as an outcome of decalcification of cementitious materials [89, 91].

Changes in gel pore volumes, specific surface area and structure of silicates are all indicating that the leaching of Portlandite is accompanied by decalcification of CSH gel. As mentioned previously, this phenomenon is noted in literature by Adenot and Buil [42].

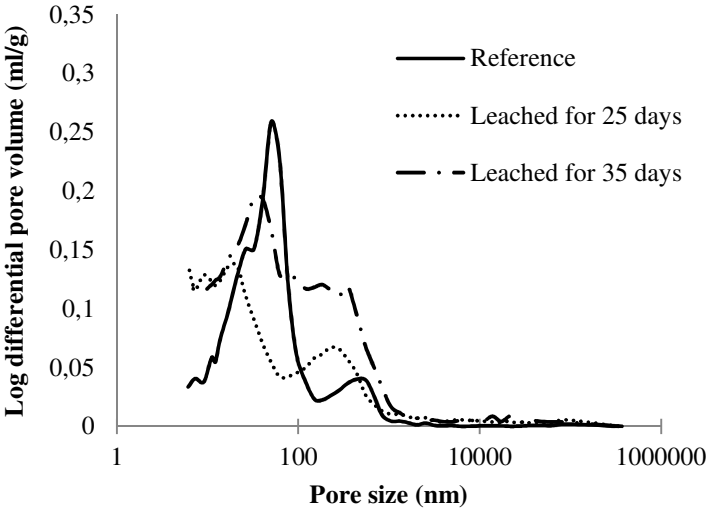

Figure 4-7. Pore size distribution results: mercury intrusion analyses. (The aged paste sample had been leached for 25 and 35 days.)

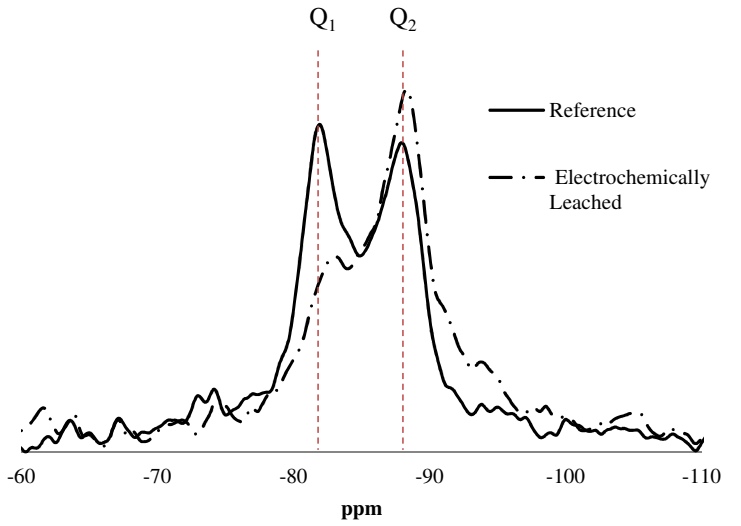

Figure 4-8. NMR results: the changes in structure of ^{29}Si after leaching

4.2.2 Freezable water

Table 4-2, presents the colorimetric results which indicate changes in the freezing ability of the water content in specimens subjected to leaching. Colorimetri analysis are reported in the literature to account for freezable water in porous cementitious materials as an indication of pore size distribution [92-94]. A larger portion of freezable water indicates a larger pore system, because the water in gel pores requires very low temperatures to freeze.

The results presented in Table 4-2 include the thawing energy obtained from colorimetric results, the freezable water calculated according to the thawing energy and heat of fusion of water as well as maximum possible heat calculated according to the total water content of specimens and heat of fusion of water. Also four parameters: A, B, C and J_1/J_2 are defined in that table. Parameter A, B and C are the total, frozen and un-frozen water content in the specimens normalized with regard to the dry weight of the specimens. The J_1/J_2 parameter is the ratio of thawing heat to maximum heat, which is an indication of the freezing ability of water. As can be seen in Table 4-2, higher B values for leached specimens show that more water was frozen in leached specimens, which is due to higher capillary pore volume in these specimens (Figure 4-6). Also the higher C values indicate more unfrozen water exists in leached specimens, which is also due to the larger gel pore volume (Figure 4-6), considering that the un-frozen water is the water in gel pores. However the increase rate of B as shown is higher than C values indicating that leaching-induced changes in capillary pores are more than in gel pores.

Table 4-2. Changes in freezing properties due to leaching

Material	Dry weight	Total water	Thawing (J_1)	Freezable water*	Max heat (J_2)*	A=Total water/dry weight	B=frozen water/dry weight	C=un-frozen water/dry weight	Freezability (J_1/J_2)
Reference paste	17,13	5,62	841	2,52	1880	0,32	0,15	0,18	0,45
Leached paste 1	8,86	3,62	584	1,75	1209	0,4	0,20	0,21	0,48
Leaced paste 2	10,43	5,87	1216	3,64	1960	0,56	0,35	0,21	0,62
Reference mortar	18,11	2,05	371	1,11	684	0,11	0,06	0,05	0,54
Leached mortar	19,28	2,95	574	1,72	988	0,15	0,09	0,06	0,58

*Freezable water= J_1/heat of fusion of water

*Max heat = water content*heat of fusion of water (334 J/g)

Accordingly the J_1/J_2-ratio indicates higher freezing ability in leached specimens. It should be noted that there is a considerable deviation in the results comparing leached sample 1 and 2, which requires further investigations to draw concrete conclusions regarding the quantified rate of changes.

4.3 Transport properties of leached specimens

4.3.1 Adsorption and diffusion

The results of the adsorption test are illustrated in Figure 4-9, and indicate that the free concentrations of cesium ions in the mixtures containing the leached cement paste were considerably lower than the mixtures that contained the reference samples. This implies that the aged cementitious materials have a greater binding potential, which is in agreement with the findings previously reported by Ochs et.al [17]. A plausible explanation for the enhanced adsorption of Cs^+ ions in the aged samples is that when almost all alkali ions and a large portion of the Ca^{2+} ions have been removed during the leaching process, a large number of negatively charged adsorption sites of silicates are made available for Cs^+ ions. On the other hand, in the case of pristine materials, the available adsorption sites for Cs^+ ions are fewer because a large portion of these sites have already been occupied by Ca^{2+}, Na^+ or K^+ ions. This is also in agreement with the measured higher specific surface area of the aged samples, as presented in Figure 4-8.

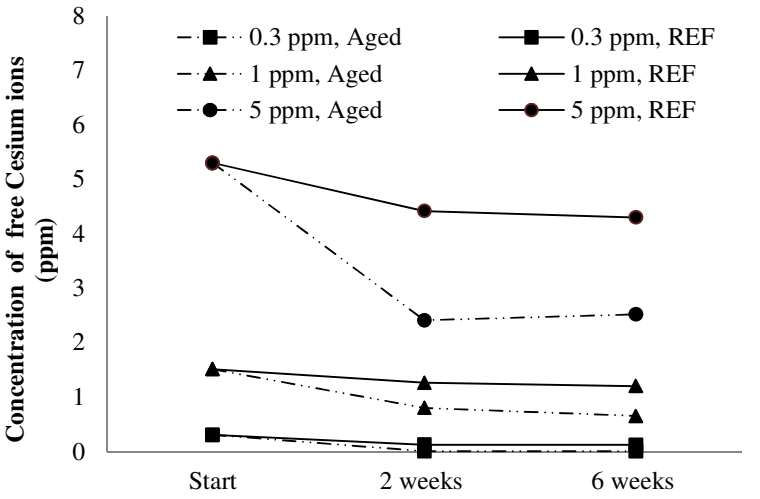

Figure 4-9. Adsorption test results

The effect of leaching on the transport properties of cementitious materials is not only due to changes in adsorption properties, but also due to changes in the ionic diffusion and pore structure of cementitious specimens [40]. The diffusion cell test results demonstrating the combined effect of changes in pore volume, diffusion and adsorption on ionic transport properties are presented in Figure 4-10. In this figure, the accumulated concentration of

diffused ions has been plotted as a function of time. As shown in the figure, the diffusion rates were higher for all the ions in the aged specimens than in the reference material. Owing to the fact that the aged specimens have a higher porosity, as demonstrated in previous sections, a higher diffusion rate can reasonably be expected. Also shown in Figure 4-10 (a), is that the diffusion rate of Cs^+ ions in an aged sample is similar to that of the Na^+ ions in a comparable sample. However, this is in contradiction to the diffusion rate in a pure salt solution in which the diffusion coefficient of Cs^+ ions is higher than that of the Na^+ ions (for a concentration of ~ 4 mol/dm^3, diffusion coefficients of 0.941 and 1.660 m^2/s are reported for NaCl and CsCl solutions respectively [95]). This may be explained by the enhanced adsorption of Cs^+ ions on the surfaces of the aged specimens, which has been demonstrated to be caused by less competition between Cs^+ and other ions for occupying the free negative sites [17]. Furthermore, considering the higher degree of hydration of the Na^+ ions compared with Cs^+ ions [80], the binding potential for Na^+ ions can be expected to be weaker. This implies that although free negative sites are available after the degradation of cementitious materials, a strong ionic binding potential is needed to fill these sites and this potential is higher for cesium ions than for sodium ions. As a result, the greater adsorption potential of Cs^+ ions decreases the diffusivity of these ions in degraded samples. In contrast, plot (b) in Figure 4-10, shows that the rate of diffusion for Cs^+ ions was relatively higher than the rate of diffusion for Na^+ ions in 0.5 M solutions. The discrepancies between 0.05 and 0.5 M solutions can be explained according to the effect of ionic concentration on binding. In a 0.05 M solution, the diffusion of Cs^+ ions decreases in comparison with a pure ionic solution and becomes nearly equal to the diffusion of Na^+ ions due to the stronger adsorption at the negatively charged surfaces, plot (a). However, in a 0.5 M solution, ionic diffusion overcomes these adsorption effects due to higher concentration gradients and as a result the diffusion of Cs^+ ions will not be affected by the adsorption effect, plot (b).Similarly, the difference between the diffusion rates of Cl^- ions in a CsCl solution and a NaCl solution will be lower in 0.05 M solutions, plot (c), than in 0.5 M solutions, plot (d). This indicates that if the diffusion coefficient of Cs^+ ions is reduced owing to the adsorption effect, the diffusion coefficient of Cl^- ions will also be affected. This is because the diffusion of cations and anions is highly coupled to maintain the electro-neutrality of the system. Therefore, a lower rate of Cs^+ ions will cause a decrease in the diffusion of chloride ions as well.

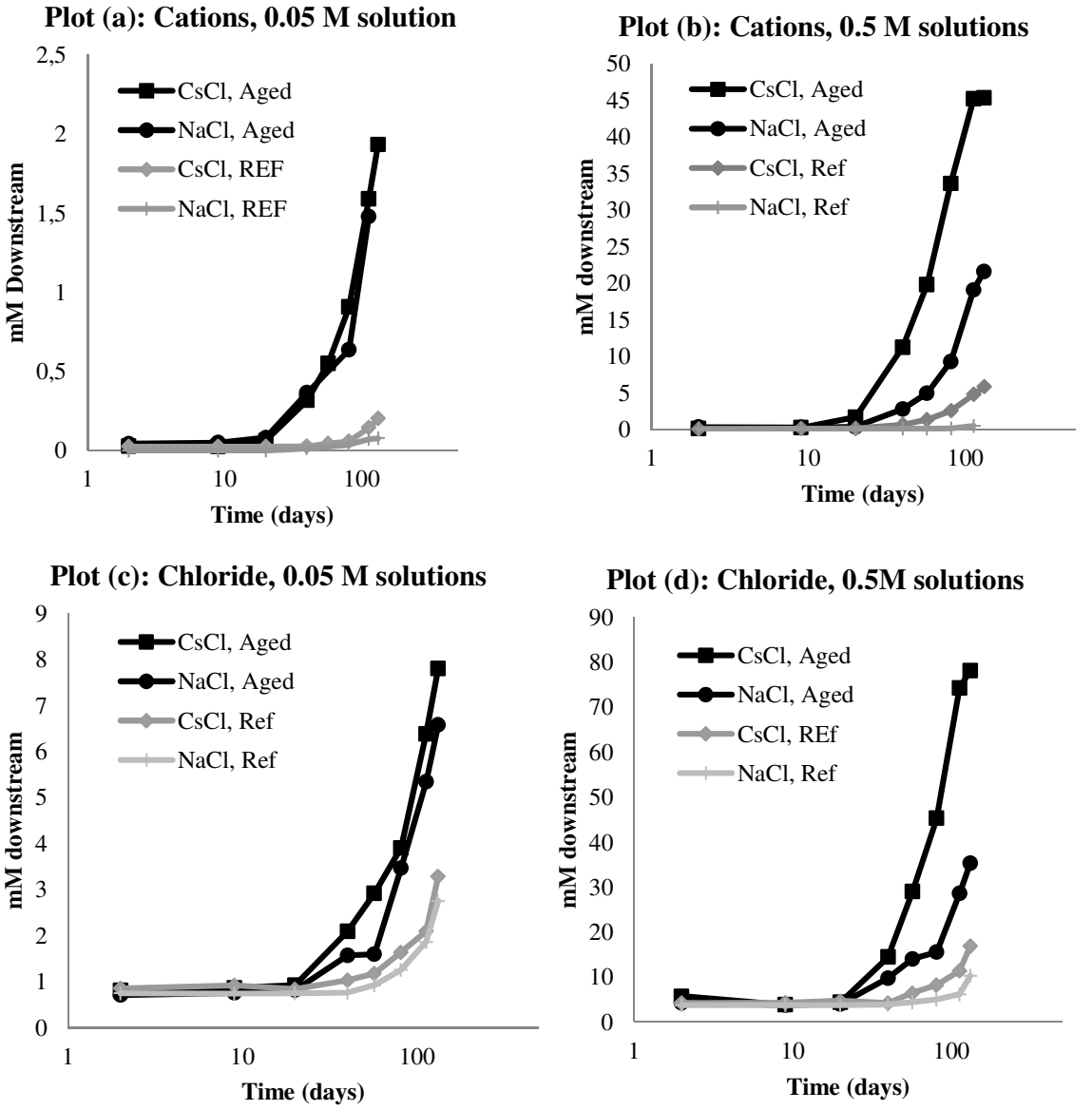

Figure 4-10. Diffusion cell test results: changes in ionic transport properties due to leaching

As presented in Figure 4-11 and paper III, it should be noted that, the changes in ionic concentration in the solution affect the ionic diffusion coefficients. It is shown in the figure that the diffusion coefficient of cations and anions differed by approximately an order of magnitude. Moreover, the diffusion coefficient value decreased (in most of cases) due to an increase in the ionic concentration of the upstream cell, which is logical, due to the friction effects between ions.

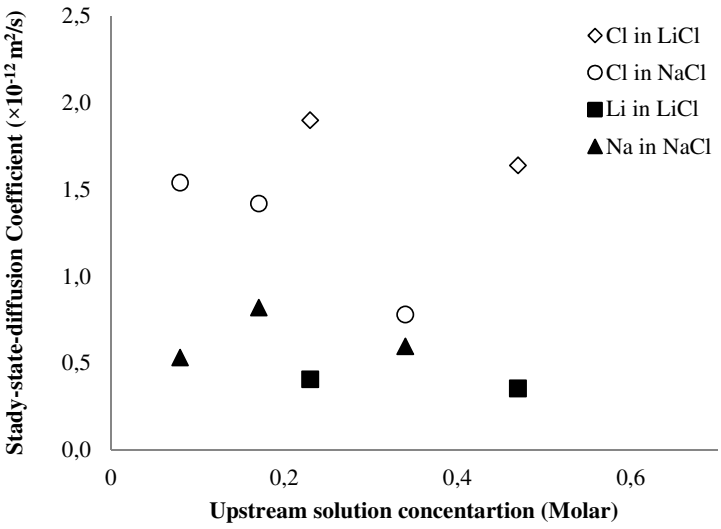

Figure 4-11. The effect of ionic concentration of upstream cell on ionic diffusion coefficient

4.3.2 Gas permeability and capillary water absorption

The capillary water absorption results representing the changes in the pore structures of the specimens are presented in Figure 4-12. As shown in the figure, capillary water absorption increased in the calcium-depleted specimens compared with the pristine material to a large extent. Considering the presented results, it can be inferred that the capillary water absorption in 24 hours increased by a factor of 4 and 2 for calcium-depleted specimens with W/C-ratios of 0.48 and 0.62, respectively. In addition, the difference in capillary water absorption between the aged specimens with different water cement ratios is relatively less than that of between reference specimens. A plausible explanation is that after leaching the pore structure becomes comparable in decalcified specimens no matter which initial W/C-ratios they had (it should be noted that according to Table 3-3 the paste volume is the same for specimens with different W/C-ratios). The change in the gas permeability coefficient, which is another representative parameter for the pore volume of cementitious materials, is presented in Figure 4-13. It is seen that the gas permeability in the calcium-depleted specimens was more than 10 times higher than that in the pristine material. This can also be explained by the larger pore volume in the specimens after decalcification.

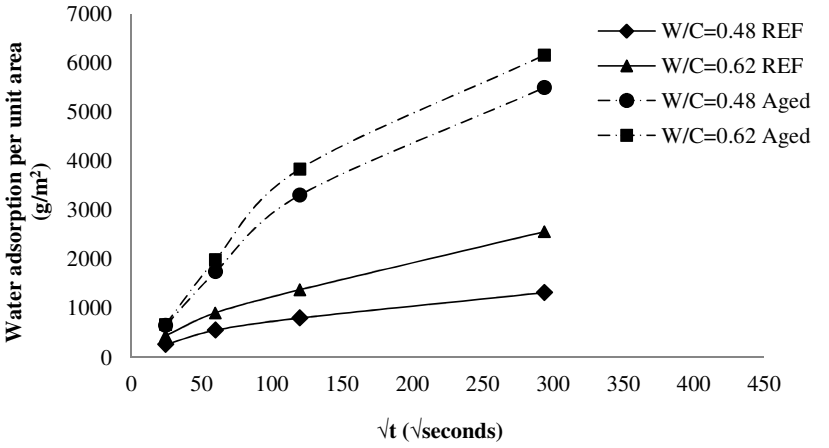

Figure 4-12. Capillary water absorption in square root of time for concrete specimens with W/C-ratios of 0.48 and 0.62 before and after leaching

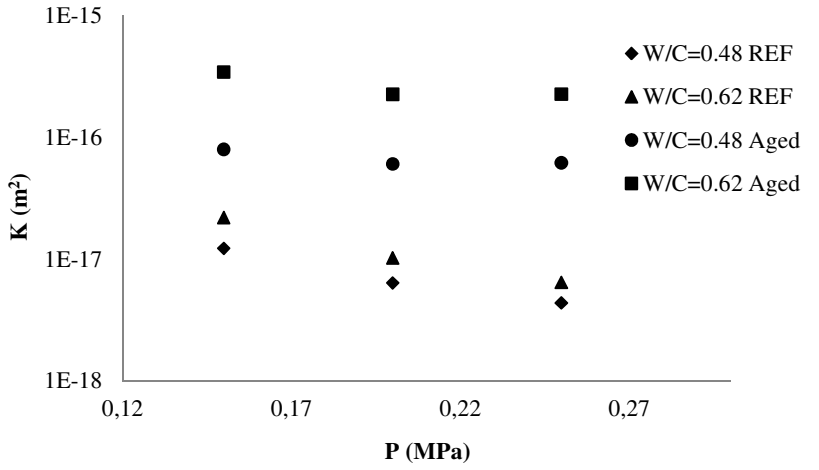

Figure 4-13. Gas permeability coefficient K as a function of applied absolute gas pressure P for concrete specimens with W/C-ratios of 0.48 and 0.62 before and after leaching

4.4 Mechanical properties of leached specimens

The mechanical properties of the concrete specimens are presented in Table 4-3. As can be seen, the average tensile strength for the specimens with a W/C-ratio of 0.48 has been reduced by up to approximately 70% due to calcium depletion, whereas the reduction in tensile strength for the specimen with a W/C-ratio of 0.62 was about 55%. Interestingly, the strength of the Ca-depleted specimens is very similar regardless of the W/C-ratios of the original specimens. Interestingly the strength reduction factors are comparable to

capillary water absorption increased factors. However, it should be noted that the repeatability of such similar factors should be further investigated to draw more concrete conclusions. The changes in the compressive strength of the mortar and paste specimens are also presented in Table 4-4. As can be seen, a relatively similar residual strength level is reached for paste and mortar specimens after leaching. The lower residual strength level in mortar and paste specimens compared to concrete specimens is due to larger paste portion in these specimens which is affected by leaching phenomenon.

Table 4-3. Average tensile and compressive strengths of concrete specimens

	Tensile strength (MPa)			**Compressive strength (MPa)**		
	Ref	**Aged**	**% decrease**	**Ref**	**Aged**	**% decrease**
W/C=0.48	10.2 ± 0.1	2.8± 0.1	72	43± 0.3	12.7± 0.1	70
W/C=0.62	5.5± 0.5	2.5± 0.1	55	30± 0.1	12.7± 0.1	58

Table 4-4. Average compressive strength results for mortar and paste specimens

		Compressive Strength (MPa)		
	W/C	**Ref**	**Aged**	**% decrease**
Mortar	0.5	38.8± 0.3	9.9± 0.3	74
Paste	0.5	21.6± 0.2	9.5± 0.1	56

The presented outcomes are in good agreement with the conclusions presented by Carde et al. (1996). In their study, they showed that the loss of strength due to the complete removal of Portlandite can be up to 70%. It has also been shown that the main contribution to the changes in strength properties is due to the leaching of Portlandite, and that the effect of CSH degradation is negligible [12, 36, 37]. An increase of up to 50 % in total pore volume of leached paste samples was demonstrated in the previous section, which clearly justifies the changes in strength properties. This indicates that when leaching propagates towards an approximate complete leaching of Portlandite, because of similar obtained pore structures, comparable strength properties can be expected in samples with different initial W/C-ratios.

Further, the Elastic modulus of the specimens, obtained as the slope of the stress-strain curves, is presented in Figure 4-14. As shown in the figure, the elastic modulus was reduced by up to 40% in both concrete specimens due to leaching.

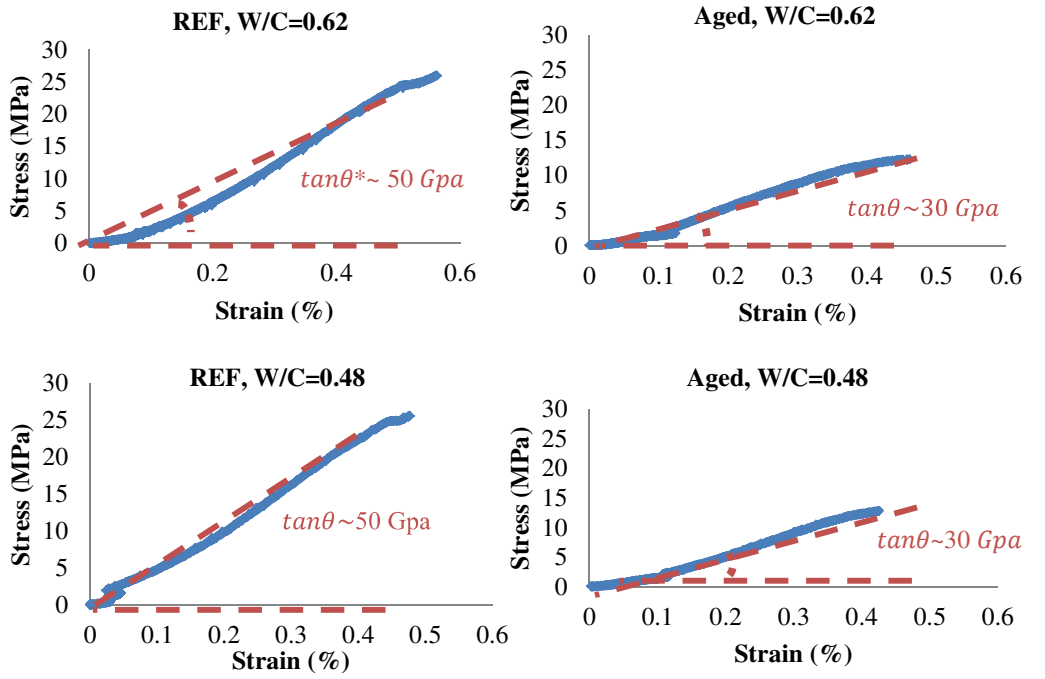

* $\tan\theta = Elastic\ modulus$

Figure 4-14. Stress-strain curves

To confirm these results, the obtained elastic modulus in terms of fundamental longitudinal frequency is also presented in Table 4-5. The results demonstrate that the reduction factor of elastic modulus due to leaching is comparable between all the cementitious materials, despite their initial W/C-ratios.

Table 4-5. Resonant frequency and calculated E-modulus of the reference and aged specimens

		F (kHz)		E (GPa)		Decrease%
		Ref	**Aged**	**Ref**	**Aged**	
Concrete	**W/C=0.48**	27.4	21.6	46.5	24.1	48
	W/C=0.62	29.3	22.1	46.5	24.6	47
Mortar	**W/C=0.5**	25.7	17.6	30.4	15.18	50
Paste	**W/C=0.5**	17.6	13.2	11.4	6.24	45

4.5 Comparability of leached specimens with degraded specimens leached with reference leaching methods

Figure 4-15 shows the longitudinal ICP-MS line scans that illustrate the changes in the Ca/Si-ratio for the specimens leached with the natural immersion test. The scanned lines as well as the leaching fronts are also illustrated in Figure 4-16. The results represent 2 and 3.5 years of leaching time. A comparison of Figure 4-15 with Figure 4-1 shows that the shape of the leaching front is comparable in the specimens leached with both natural immersion and electrochemical migration method.

As shown in Figure 4-16, the Ca/Si-ratio representative curve has been categorized into 4 zones. In Zones 1 and 2, the Ca/Si-ratio shows that the Portlandite has been leached. However, in Zone 2 there is a gradient in the Ca/Si-ratio for the specimen leached for 2 years, and the Ca/Si-ratio increased in Zone 3. This indicates that the leaching front, after 2 years of leaching, is approximately up to Zone 2 (=6 mm) which propagates to 11 mm after 3.5 year.

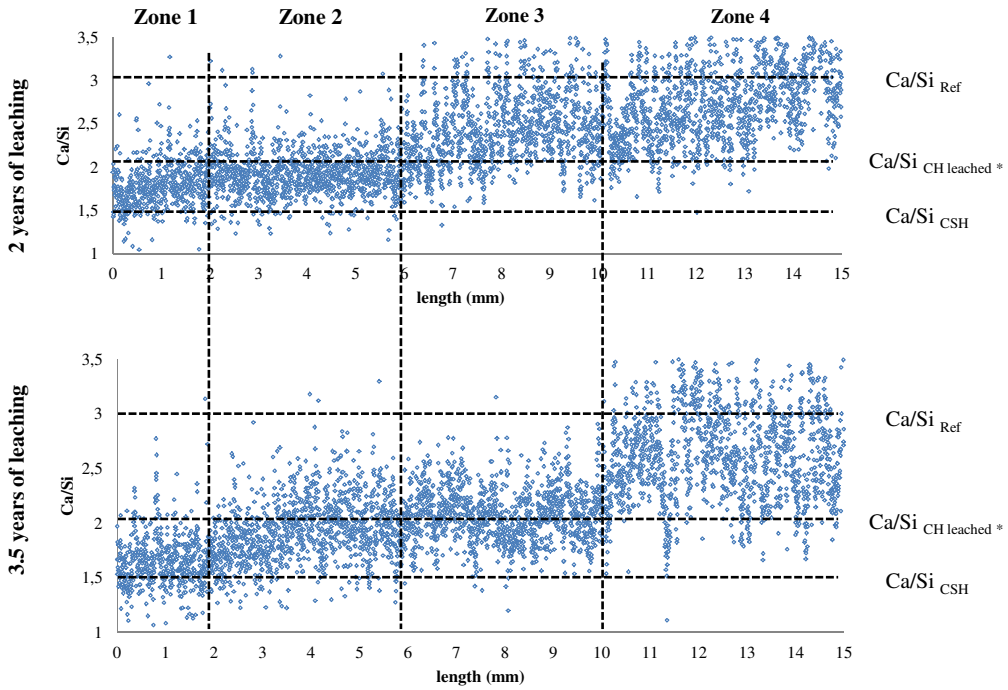

*Ca/Si $_{CH\ leached}$: Ca/Si ratio corresponding to Ca/Si $_{CSH + other\ hydrates}$ after leaching of portlandite

Figure 4-15. LA-ICP-MS analysis of specimens leached with the natural immersion test

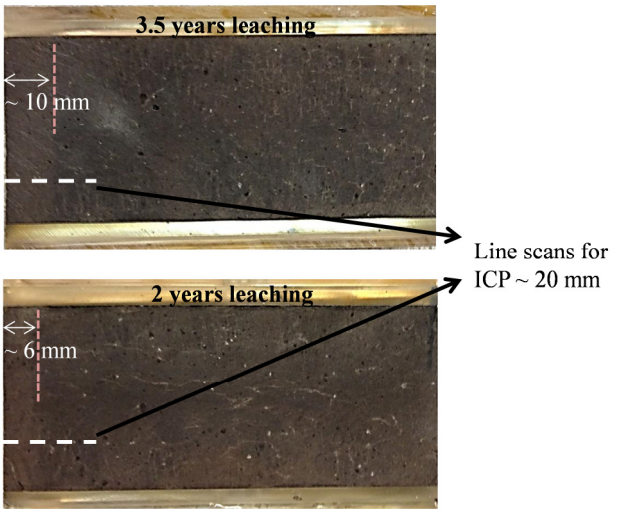

Figure 4-16. Visual leaching front and ICP-MS scan lines for specimens leached with the natural immersion test

The demonstration of the preferential leaching of Portlandite in the specimens with a leaching front of 6 and 10 mm after 2 and 3.5 years of leaching, respectively, is presented in Figure 4-17. The temperature-induced mass changes did not indicate any Portlandite peak in the leached samples.

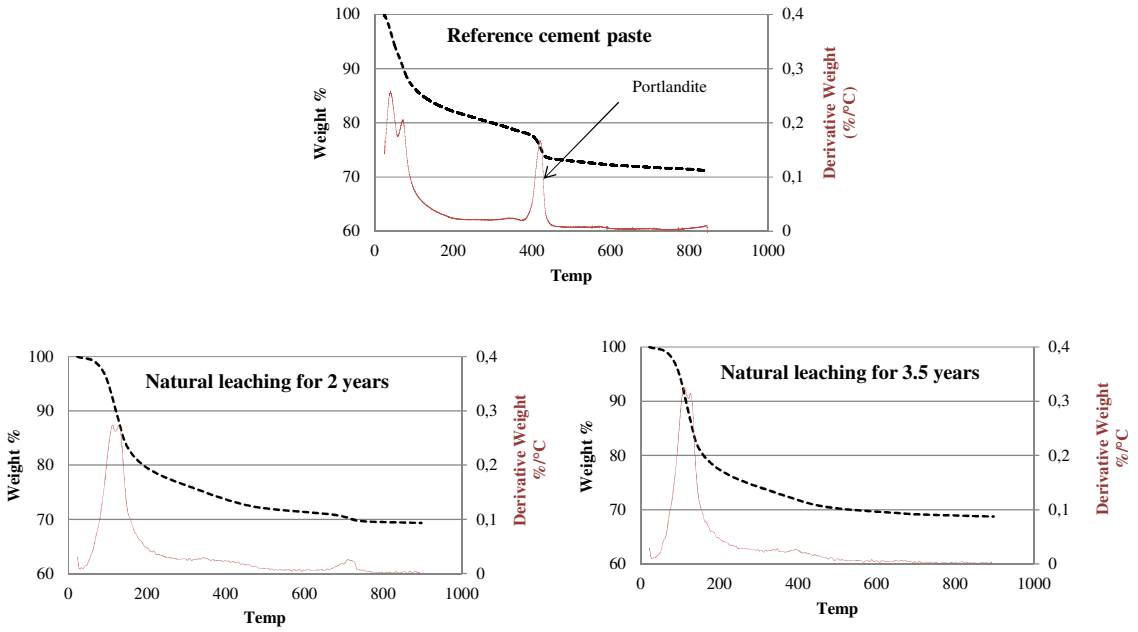

Figure 4-17. Thermogravimetric analysis of samples leached for 2 and 3.5 years with the natural immersion test compared with un-leached reference material.

The results concerning the preferential leaching of Portlandite in samples leached with other reference accelerated leaching methods are presented in Figure 4-18. As can be seen, all methods are enabling the preferential leaching of Portlandite. However, it should be noted that as the leaching level is different in these samples, no other conclusion rather than comparability in preferential leaching of Portlandite concerning the leaching function of these methods is made.

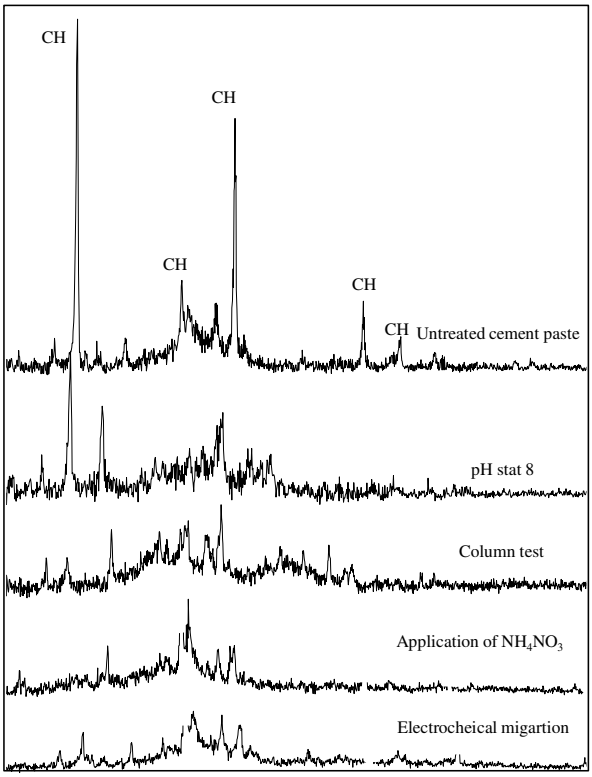

.

Figure 4-18. XRD results for decalcified cement paste samples leached with proposed accelerated leaching methods in literature and electrochemical migration method.

Moreover, as mentioned the progression of degradation in CSH gel is determined with respect to NMR results for ^{29}Si, representing changes in the structure of calcium silicate hydrates after. The sample for analysis of the changes in naturally leached specimens were taken from outer most 2 mm of the leaching front and the case of electrochemically leached specimens the sample represents the obtained 75 mm depletion front after 53 days of leaching. As shown in Figure 4-19, the Q_1 peaks are decreasing for both leached samples while the increase in the intensity of Q_2 peaks indicates polymerization of silicates (longer chains [91]). This demonstrates the comparability of decalcified specimens leached with both electrochemical and natural methods, in terms of changes in the structure of CSH gel.

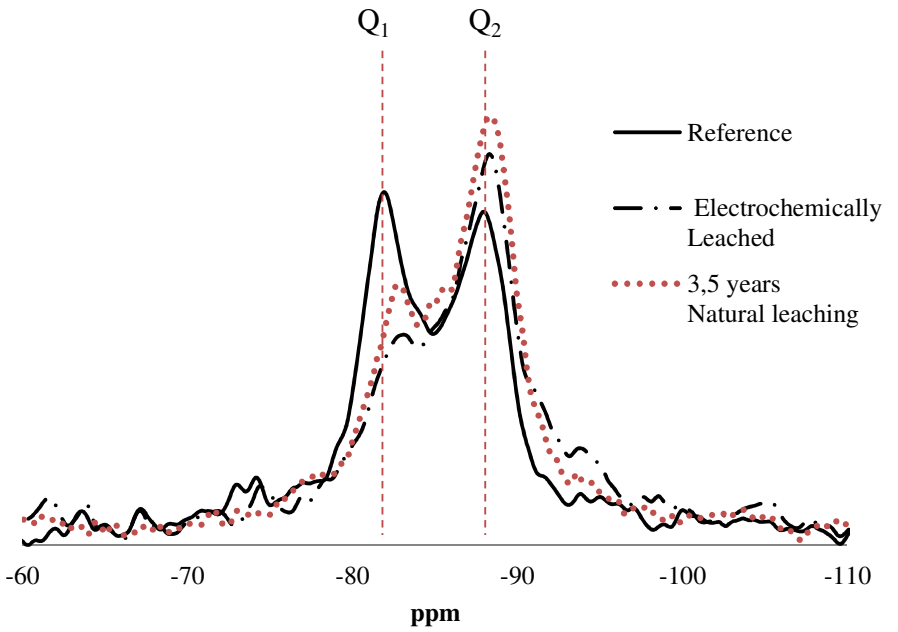

Figure 4-19. NMR results: the changes in structure of ^{29}Si after leaching

Moreover, results from BET analysis (for similar samples as for NMR analysis), indicated a significantly higher specific surface area in leached specimens degraded with both electrochemical migration and natural leaching methods. According to several sets of experimental results the specific surface area was approximately 50, 90 and 85 m^2/g for reference, electrochemically leached and naturally leached samples, respectively. Accordingly the comparability of leached specimens with both methods in terms of changes in specific surface area is demonstrated.

5 Conclusions

The effect of decalcification on the properties of cementitious materials was investigated. The aim was to provide experimental databases to improve predictions regarding the functionality of cementitious barriers in nuclear waste repositories. To fulfill the lack of a sufficient accelerating test method to produce degraded cementitious specimens of flexible size, the electrochemical migration method was developed. The manufactured decalcified specimens were characterized with respect to chemical, mineralogical, physical, transport and mechanical properties. The comparability of properties with the characteristics of specimens produced with natural immersion was investigated and further possibilities for continued research are accounted for. The concluding remarks are presented below.

I. Electrochemical migration test method

The electrochemical migration method as a test method that accelerates the decalcification of cementitious materials was developed and a recommended test procedure was proposed in this study. The acceleration was obtained as a result of higher dissolution rate of calcium hydroxides, by application of ammonium nitrate, as well as faster transport of calcium ions, by an external electrical field. The specific conclusions regarding this method are as follows:

- With the application of the electro-chemical migration method the ageing of cementitious materials is driven by the migration function at an ageing rate far higher than that of the natural leaching rate.
- Calcium transport has an average transport number of 0.2, indicating that calcium ions are available in the pore solution during the leaching period and at least 20% of the applied charge is carried by these ions.
- The method can enable leaching of specimens of flexible sizes, and the addition of aggregates does not interfere with the leaching process.
- Leaching level can be predicted by monitoring the leached calcium content in catholyte solution.

- With a current density of 125-130 A/m^2, a depletion depth of 75 mm was obtained after 53 days of leaching with the application of the electrochemical migration method. The dissolution front corresponds to the complete leaching of Portlandite, with a certain degree of phase changes in the CSH gel (Ca/Si<1.5) of the material.

II. Characteristics of degraded specimens

The changes in the characteristics of cementitious specimens due to leaching induced by the application of the electrochemical migration method were investigated. The characterizations of specimens in terms of chemical and mineralogical properties as well as changes in pore structure of specimens were performed by means of various instrumental analysis: XRD, XRF, IC, LA-ICP-MS, SEM/EDX, MIP, BET/BJH, TGA/DSC. The changes in properties such as diffusion and adsorption, strength and modulus, permeability and water absorption as well as freezable water were also studied. The credibility of the electrochemically degraded specimens was also accounted for by comparing the characterization outcomes with properties of degraded specimens leached with the natural leaching method and other methods proposed in the literature. These investigations led to the following conclusions:

- Similar to natural leaching and other results reported in the literature, ageing using the electrochemical migration method causes the dissolution of Portlandite followed by progressive decalcification of the CSH gel in the material.
- Probable leaching-induced precipitations occur when using the electrochemical migration method, similar to naturally leached specimens. However, with longer leaching times these precipitations eventually leach out.
- The specific surface area of the calcium-depleted paste specimens leached with both natural and electrochemical leaching methods increased considerably after leaching. This is due to silicate polymerization which was demonstrated by NMR analysis.
- The cumulative pore volume of the calcium-depleted paste specimen increased considerably, compared with that of the pristine material. This caused a significant increase in the ionic diffusion rate of the aged samples. A larger pore volume for pore sizes lower than 100 nm indicates that the changes in pore structure after

degradation occur not only in the larger pores but also in the gel pores of the material.

- The aged cementitious samples exhibited a higher binding potential for Cs^+ ions. As almost all the alkali ions and a large portion of the Ca^{2+} ions had been leached from the sample, a large number of negatively charged adsorption sites were created for Cs^+ ions.
- The combined effect of binding potential, porosity and ionic diffusion should be considered when assessing the transport properties of ions.
- Leaching of Portlandite causes considerable changes in the physical and mechanical properties of concrete specimens, primarily due to an increase in pore volume. This would cause up to a 70% decrease in the mechanical strength and 40% decrease in the elastic modulus of the material.
- The larger pore volume that occurs after calcium depletion in concrete specimens causes more than 10 times higher gas permeability and at least a 3 times higher chloride migration rate.
- The properties of the concrete specimens after complete leaching of Portlandite were found to be similar no matter which initial water cement ratios the specimens had. This is, to a great extent, due to similar pore structures in the concrete specimens after leaching.
- Leaching seems to increase the freezing ability of pore water in cementitious materials. This could be due to the larger pore structure that occurs after leaching.
- The leaching front with the application of the electrical migration method was similar to the leaching front in specimens leached with the natural immersion test in terms of shape, preferential leaching of Portlandite and polymerization of silicates.

6 Future Work

The outcomes of this project can be further utilized to pinpoint the most important factors to be considered in long-term predictions of the degradation caused by calcium leaching. These outcomes and further detailed investigations can be used as databases for modeling the leaching process of cementitious materials in long-term perspectives.

The electrochemical migration method has proven to be a very effective method for producing samples of flexible size with a high leaching rate, however, similar to any other acceleration method, further investigations are needed to confirm the comparability of the produced degraded samples with naturally leached materials. Moreover, the ageing function of the method and the acceleration rate are important parameters to be clarified.

Quantitative adsorption and diffusion tests for cementitious materials with better precision are needed in order to supply accurate databases for service life modeling. Nevertheless, producing aged specimens by the electrochemical acceleration method and simulating the adsorption and diffusion process in several leaching levels are necessary steps before any numerical modeling.

Further studies of degradation of CSH gel after complete leaching of Portlandite are needed in order to predict the entire service life of repositories of nuclear waste.

7 Appendix: Recommended manual for electrochemical migration test method

7.1 Scope

This manual demonstrates a step by step experimental procedure for applying the electrochemical migration method in order to produce calcium leached cylindrical cementitious specimens of flexible sizes.

7.2 Apparatus

7.2.1.1 Sealants

7.2.1.1.1 Asphalt tape:

An asphalt tape (type BITUTHENE) or a similar product providing elasticity should be used to seal the curved surface of specimen. 200 mm width for the elastic tape is recommended.

7.2.1.1.2 Plexiglas

A plexiglas tube with an outer diameter size similar to the specimen's diameter is required.

7.2.1.1.3 Clamper

Stainless still clamper should be used

7.2.1.2 Electrodes

7.2.1.2.1 Anode

0.5 mm thick Titanium mesh, equipped with a plastic spacer

7.2.1.2.2 Cathode/plastic support

0.5 mm thick stainless steel plate and a plastic support prepared according to NT BUILD 492 [76]

7.2.1.3 Power supply

Capable of supplying a voltage of 100 V and a constant current of up to 1-2 A

7.2.1.4 Reservoirs

7.2.1.4.1 Catholyte reservoir

Plastic box with a capacity of at least 20 liters

7.2.1.5 REAGENTS

7.2.1.5.1 Anolyte

2 M Lithium Hydroxide

7.2.1.5.2 Catholyte

0.3 M ammonium nitrate

7.3 Test preparation

125-130 A/m^2_{paste} of current density should be applied to the specimen to reach to an efficient leaching rate without inducing thermal damages.

Considering a paste specimen of size Ø50×75 mm as an example, with application of such a current density, a current of 250 mA and a maximum potential of 100 volts is expected which corresponds to 25 W of electrical power.

In order to calculate the needed current and expected potential and applied power:

1) Calculate the cross-sectional area of the specimen, A (m^2)
2) Consider the volume percentage of the paste in the specimen, %VP
3) Calculate the cross-sectional area of the paste content: $A \times \%V_p = A_p$
4) Calculate the needed current: $I(A) = A_P \times 127$
5) Start the test and read the potential on power supply
6) Calculate the power: $P = V \times I$
7) If P > 25 W decrease the current density by 75% and register the potential and recalculate the power. Continue until the calculated power does not exceed 25 W.

7.4 Test procedure

1) Seal the cylindrical cementitious specimen with the asphalt tape and then tighten it by the clampers.
2) The asphalt tape used to seal the curved surface of the specimen should be extruded to provide an empty volume of about 200-300 ml to be used as the anolyte reservoir, Figure 7-1.
3) In case of utilizing a specimen with a diameter larger than 50 mm it is recommended to place a Plexiglas tube on top of the specimen according to Figure 7-2. The asphalt tape should be used to assemble them together while also sealing the specimens curved surface and sealant should be tightened with the clampers.
4) Fill up to one third of the anolyte reservoir with a 2 M LiOH solution.
5) Place aside the assembled set-up for 5-10 minutes to check possibility of leakage. In case of leakage, tight the clampers and wait for mere 10-15 minutes to make sure there is no more leakage.
6) Fill the catholyte reservoir with 10 liters of 0.3 M ammonium nitrate solution.
7) Place the plastic support/cathode set-up inside the catholyte reservoir and place the specimen on the plastic support according to Figure 7-3.
8) Insert the anode in to the anolyte reservoir.
9) Connect the anode to + pole and the cathode to the – pole of the power supply.
10) Adjust the current to the calculated required current (according to previous section) and set it to constant.
11) If the initial potential is much higher than the calculated values, reduce the current slowly to maintain a power lower than 25 W.
12) The regents should be recharged according to section 7.5.
13) The accumulated calcium content in the catholyte solution should be measured frequently to account for the desired leaching state. For a current density of 125-130 A/m^2_{paste}, approximately 53 days of experimental time is needed to reach to complete leaching of Portlandite.

14) When the experimental time (the desired leaching state) is reached, the experiment should be stopped and the specimens should be disassembled and sealed with a thick parafilm.

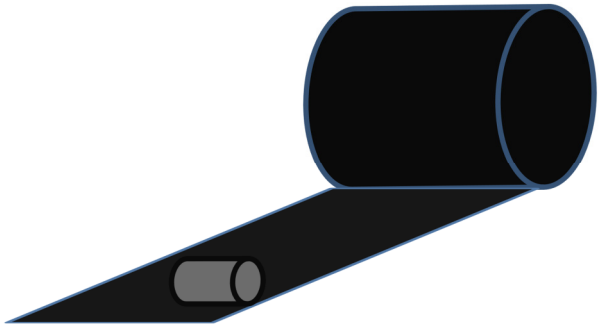

Figure 7-1. sealant: asphalt tape.

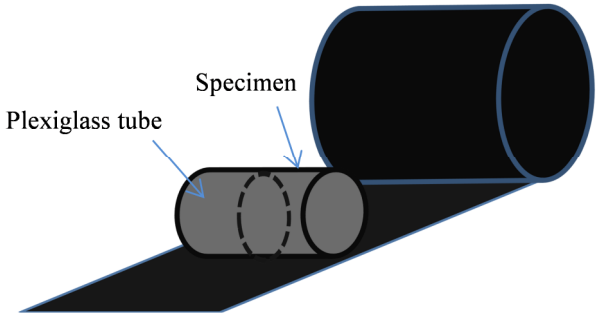

Figure 7-2. sealing method for specimens of diameter larger than 50 mm.

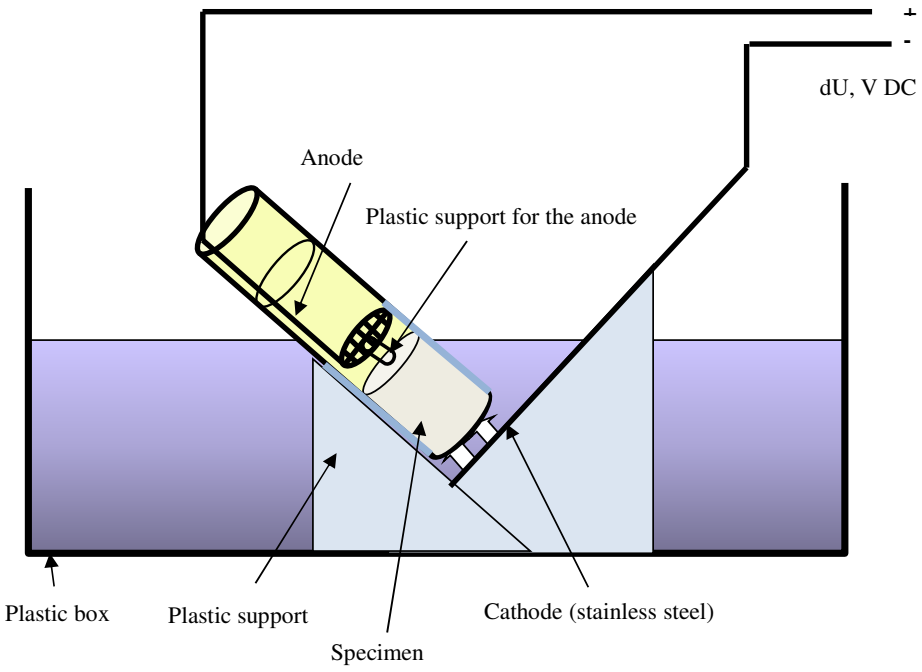

Figure 7-3. location of the specimen and the set-up design for anode and cathod

7.5 Recharging reagents

Calculate the required quantities of the salts for every 24 hours of recharging according to:

$$m_{NH_4NO_3} = 71 \cdot I$$

$$m_{LiOH} = 22 \cdot I$$

where,

m: mass of substance (grams)

I: Applied Current (A)

The calculated amounts can be rounded up to a value that can be measured with precision of 1 gram.

8 Bibliography

[1] A. Adamantiades, I. Kessides, Nuclear power for sustainable development: Current status and future prospects, Energy Policy, 37 (2009) 5149-5166.

[2] M.I. Ojovan, W.E. Lee, 20 - Nuclear Waste Disposal, in: M.I.O.E. Lee (Ed.) An Introduction to Nuclear Waste Immobilisation (Second Edition), Elsevier, Oxford, 2014, pp. 321-335.

[3] M. Atkins, F.P. Glasser, Application of portland cement-based materials to radioactive waste immobilization, Waste Management, 12 (1992) 105-131.

[4] C. Langton, D. Kosson, review of mechanistic understanding and modeling and uncertainty analysis methods for predicting cementitious barriers performance, 2009.

[5] U.R. Berner, Evolution of pore water chemistry during degradation of cement in a radioactive waste repository environment, Waste Management, 12 (1992) 201-219.

[6] E.J. Reardon, Problems and approaches to the prediction of the chemical composition in cement/water systems, Waste Management, 12 (1992) 221-239.

[7] E. Revertegat, C. Richet, P. Gégout, Effect of pH on the durability of cement pastes, Cement and Concrete Research, 22 (1992) 259-272.

[8] K. Yokozeki, K. Watanabe, N. Sakata, N. Otsuki, Modeling of leaching from cementitious materials used in underground environment, Applied Clay Science, 26 (2004) 293-308.

[9] J. Trägårdh, B. Lagerblad, Leaching of 90-year old concrete in contact with stagnant water, SKB Technical Report TR 98-11, Swedish Nuclear fuel and Waste management, 1998.

[10] A. Sellier, L. Buffo-Lacarrière, M.E. Gonnouni, X. Bourbon, Behavior of HPC nuclear waste disposal structures in leaching environment, Nuclear Engineering and Design, 241 (2011) 402-414.

[11] H. Saito, S. Nakane, S. Ikari, A. Fujiwara, Preliminary experimental study on the deterioration of cementitious materials by an acceleration method, Nuclear Engineering and Design, 138 (1992) 151-155.

[12] H. Saito, A. Deguchi, Leaching tests on different mortars using accelerated electrochemical method, Cement and Concrete Research, 30 (2000) 1815-1825.

[13] J.-S. Ryu, N. Otsuki, H. Minagawa, Long-term forecast of Ca leaching from mortar and associated degeneration, Cement and Concrete Research, 32 (2002) 1539-1544.

[14] J. Pommersheim, J. Clifton, Prediction of concrete service-life, Materials and Structures, 18 (1985) 21-30.

[15] W. Pfingsten, M. Shiotsuki, Modeling a Cement Degradation Experiment by a Hydraulic Transport and Chemical Equilibrium Coupled Code, Mat. Res. Soc. Symp, 1996.

[16] C.L. Page, Ø. Vennesland, Pore solution composition and chloride binding capacity of silica-fume cement pastes, Mat. Constr., 16 (1983) 19-25.

[17] M. Ochs, I. Pointeau, E. Giffaut, Caesium sorption by hydrated cement as a function of degradation state: Experiments and modelling, Waste Management, 26 (2006) 725-732.

[18] V.H. Nguyen, H. Colina, J.M. Torrenti, C. Boulay, B. Nedjar, Chemo-mechanical coupling behaviour of leached concrete: Part I: Experimental results, Nuclear Engineering and Design, 237 (2007) 2083-2089.

[19] H.S.a.S. Nakane, Comparison between Diffusion Test and Electromechanical Acceleration Test for Leaching Degradation of Cement Hydration Products, Materials Journal, 96 (1999) 208-212.

[20] N. Marinoni, A. Pavese, M. Voltolini, M. Merlini, Long-term leaching test in concretes: An X-ray powder diffraction study, Cement and Concrete Composites, 30 (2008) 700-705.

[21] Y. Maltais, E. Samson, J. Marchand, Predicting the durability of Portland cement systems in aggressive environments—Laboratory validation, Cement and Concrete Research, 34 (2004) 1579-1589.

[22] M. Mainguy, C. Tognazzi, J.-M. Torrenti, F. Adenot, Modelling of leaching in pure cement paste and mortar, Cement and Concrete Research, 30 (2000) 83-90.

[23] B. Lagerblad, Leaching Performance of Concrete Based on Studies of Sample from Old Concrete Constructions SKB Technical Report TR-01-27, Swedish Nuclear Fuel and Waste Management 2001.

[24] L.-O. Höglund, Project SAFE: Modeling of long-term concrete degradation processes in the Swedish SFR repository, SKB Report, Svensk Kärnbränslehantering AB, 2001.

[25] M. Hinsenveld, A Shrinkage Core Model as a Fundamental Representation of Leaching Mechanism in Cement Stablized Waste, Department of Civil and Environmental Engineering, University of Cincinnati, Cincinnati, OH, 1992.

[26] F.H. Heukamp, F.J. Ulm, J.T. Germaine, Mechanical properties of calcium-leached cement pastes: Triaxial stress states and the influence of the pore pressures, Cement and Concrete Research, 31 (2001) 767-774.

[27] K. Haga, S. Sutou, M. Hironaga, S. Tanaka, S. Nagasaki, Effects of porosity on leaching of Ca from hardened ordinary Portland cement paste, Cement and Concrete Research, 35 (2005) 1764-1775.

[28] A. Gordon, Safety analysis SFR 1, Long-term safety SKB Rapport R-08-130, December 2008.

[29] C. Gervais, A.C. Garrabrants, F. Sanchez, R. Barna, P. Moszkowicz, D.S. Kosson, The effects of carbonation and drying during intermittent leaching on the release of inorganic constituents from a cement-based matrix, Cement and Concrete Research, 34 (2004) 119-131.

[30] P. Faucon, P. Le Bescop, F. Adenot, P. Bonville, J.F. Jacquinot, F. Pineau, B. Felix, Leaching of cement: Study of the surface layer, Cement and Concrete Research, 26 (1996) 1707-1715.

[31] P. Faucon, F. Adenot, J.F. Jacquinot, J.C. Petit, R. Cabrillac, M. Jorda, Long-term behaviour of cement pastes used for nuclear waste disposal: review of physico-chemical mechanisms of water degradation, Cement and Concrete Research, 28 (1998) 847-857.

[32] G. Fagerlund, Predicting the service life of concrete structures, Engineering Foundation Conference on Characterization and Performance Prediction of Cement and ConcreteUnited Engineering Trustees, Inc., New York, 1983.

[33] M. Emborg, J.E. Jonasson, S. Knutsson, Long-term stability due to freezing and thawing of concrete and bentonite at the disposal of low and intermediate level nuclear waste in SFR 1 (in Swedish), SKB Technical Report R-07-60, Swedish Nuclear and Waste Management Company 2007.

[34] J. Clifton, Predicting the remaining service life of concrete, U.S. Department of Commerce, National Institute of Standards and Technology, Gaithersburg, USA, 1991.

[35] Y.S. Choi, E.I. Yang, Effect of calcium leaching on the pore structure, strength, and chloride penetration resistance in concrete specimens, Nuclear Engineering and Design, 259 (2013) 126-136.

[36] C. Carde, R. François, J.-M. Torrenti, Leaching of both calcium hydroxide and C-S-H from cement paste: Modeling the mechanical behavior, Cement and Concrete Research, 26 (1996) 1257-1268.

[37] C. Carde, R. François, Effect of the leaching of calcium hydroxide from cement paste on mechanical and physical properties, Cement and Concrete Research, 27 (1997) 539-550.

[38] C. Carde, G. Escadeillas, R. François, Use of ammonium nitrate solution to simulate and accelerate the leaching of cement pastes due to deionized water, Magazine of Concrete Research, 49 (1997) 295-301.

[39] C. Alonso, M. Castellote, I. Llorente, C. Andrade, Ground water leaching resistance of high and ultra high performance concretes in relation to the testing convection regime, Cement and Concrete Research, 36 (2006) 1583-1594.

[40] Y. Albinsson, K. Andersson, S. Börjesson, B. Allard, Diffusion of radionuclides in concrete and concrete-bentonite systems, Journal of Contaminant Hydrology, 21 (1996) 189-200.

[41] K.N.V. Adinarayana, P. Sasidhar, V. Balasubramaniyan, Modelling of calcium leaching and its influence on radionuclide migration across the concrete engineered barrier in a NSDF, Journal of Environmental Radioactivity, 124 (2013) 93-100.

[42] F. Adenot, M. Buil, Modelling of the corrosion of the cement paste by deionized water, Cement and Concrete Research, 22 (1992) 489-496.

[43] P. Domone, J. Illistone, Construction Materials, Their Nature and Behaviour, 4th. ed.2010.

[44] R.H. Bogue, Chemistry of Portland Cement Van Nostrand Reinhold, New York, 1995.

[45] T.C. Powers, Structure and Physical Properties of Hardened Portland Cement Paste, Journal of the American Ceramic Society, 41 (1958) 1-6.

[46] H.F.W. Taylor, cement chemistry, 1997.

[47] H.F.W. Taylor, Proposed structure for calcium silicate hydrate gel, Journal of the American Ceramic Society, 69 (1986) 464-467.

[48] E. Henderson, J.E. Bailey, Sheet-like structure of calcium silicate hydrates, Journal of Materials Science, 23 (1988) 501-508.

[49] I.G. Richardson, G.W. Groves, Models for the composition and structure of calcium silicate hydrate (CSH) gel in hardened tricalcium silicate pastes, Cement and Concrete Research, 22 (1992) 1001-1010.

[50] H. Van Damme, R.J.M. Pellenq, F.J. Ulm, Chapter 14.3 - Cement Hydrates, in: B. Faïza, L. Gerhard (Eds.) Developments in Clay Science, Elsevier2013, pp. 801-817.

[51] J.J. Thomas, H.M. Jennings, A.J. Allen, the surface area of hardened cement paste as measured by various techniques, Concrete Science and Engineering, 1 (1999) 45 - 64.

[52] P. Brown, J. Bothe Jr, The system CaO-Al2O3-CaCl2-H2O at 23±2 °C and the mechanisms of chloride binding in concrete, Cement and Concrete Research, 34 (2004) 1549-1553.

[53] P.W. Brown, S. Badger, The distributions of bound sulfates and chlorides in concrete subjected to mixed NaCl, MgSO4, Na2SO4 attack, Cement and Concrete Research, 30 (2000) 1535-1542.

[54] F. Barberon, V. Baroghel-Bouny, H. Zanni, B. Bresson, J.-B. d'Espinose de la Caillerie, L. Malosse, Z. Gan, Interactions between chloride and cement-paste materials, Magnetic Resonance Imaging, 23 (2005) 267-272.

[55] E.P. Nielsen, D. Herfort, M.R. Geiker, Binding of chloride and alkalis in Portland cement systems, Cement and Concrete Research, 35 (2005) 117-123.

[56] F.P. Glasser, A. Kindness, S.A. Stronach, Stability and solubility relationships in AFm phases: Part I. Chloride, sulfate and hydroxide, Cement and Concrete Research, 29 (1999) 861-866.

[57] P. Henocq, E. Samson, J. Marchand, Portlandite content and ionic transport properties of hydrated C3S pastes, Cement and Concrete Research, 42 (2012) 321-326.

[58] J.J. Beaudoin, V.S. Ramachandran, R.F. Feldman, Interaction of chloride and C□S□H, Cement and Concrete Research, 20 (1990) 875-883.

[59] L. Tang, L.-O. Nilsson, Chloride binding capacity and binding isotherms of OPC pastes and mortars, Cement and Concrete Research, 23 (1993) 247-253.

[60] O. L, Höglund, A.Bengston, Progress Report SFR 91-06, Some Chemical and Physical Progress Related to The Long-Term Performance of The SFR repository, KEMAKTA Consultants Co. Stockholm, October 1991.

[61] B.B. Hope, J.A. Page, J.S. Poland, The determination of the chloride content of concrete, Cement and Concrete Research, 15 (1985) 863-870.

[62] A.C. Garrabrants, F. Sanchez, D.S. Kosson, Changes in constituent equilibrium leaching and pore water characteristics of a Portland cement mortar as a result of carbonation, Waste Management, 24 (2004) 19-36.

[63] M.D. Cohen, Theories of expansion in sulfoaluminate - type expansive cements: Schools of thought, Cement and Concrete Research, 13 (1983) 809-818.

[64] P.K. Mehta, Mechanism of sulfate attack on portland cement concrete - Another look, Cement and Concrete Research, 13 (1983) 401-406.

[65] I. Odler, M. Gasser, Mechanism of sulfate expansion in hydrated Portland cement, Journal of the American Ceramic Society, 71 (1988) 1015-1020.

[66] M. Hinsenveld, A Shrinkage Core Model as a Fundamental Representation of Leaching Mechanism in Cement Stablized Waste, Doctoral Thesis, Department of Civil and Environmental Engineering, University of Cincinnati, Cincinnati, OH, 1992.

[67] ASTM C1308-95: Standard Test Method for Accelerated Leach Test for Diffusive Releases from Solidified Waste and a Computer Program to Model Diffusive, Fractional Leaching from Cylindrical Waste Forms, (2001).

[68] ANSI/ANS-16.1: Measurement of the Leachability of Solidified Low-Level Radioactive Wastes by a Short-Term Test Procedure.

[69] ISO/TS 21268-2:2007: Leaching procedures for subsequent chemical and ecotoxicological testing of soil and soil materials

[70] F.H. Wittmann, Corrosion of Cement-Based Materials under the Influence of an Electric Field, Materials Science Forum, 247 (1997) 107-126.

[71] G. Gustafson, Hagström, M. and Abbas, Z, Beständighet av cementinjektering, FOU.Väst Underhall av berganläggningar, Avd.f.geology och geoteknik, Chalmers teckniska högskola., 2008.

[72] O. Peyronnard, M. Benzaazoua, D. Blanc, P. Moszkowicz, Study of mineralogy and leaching behavior of stabilized/solidified sludge using differential acid neutralization analysis: Part I: Experimental study, Cement and Concrete Research, 39 (2009) 600-609.

[73] M. Castellote, I. Llorente, C. Andrade, C. Alonso, Accelerated leaching of ultra high performance concretes by application of electrical fields to simulate their natural degradation, Materials and Structures, 36 (2003) 81-90.

[74] F.-J. Ulm, E. Lemarchand, F.H. Heukamp, Elements of chemomechanics of calcium leaching of cement-based materials at different scales, Engineering Fracture Mechanics, 70 (2003) 871-889.

[75] L. Tang, Electrically accelerated methods for determining chloride diffusivity in concrete - Current development, Magazine of Concrete Research, 48 (1996) 173-179.

[76] NT BUILD 492, Concrete, Mortar and Cement-based Repair Materials: Chloride Migration Coefficient from Non-steady-state Migration Experiments, , 1999.

[77] P. Cronstrand, A. Babaahmadi, L. Tang, Z. Abbas, Electrochemical leaching of cementitious materials: an experimental and theoretical study, 1st International Symposium on Cement-Based Materials for Nuclear Wastes, NUWCEM 2011.

[78] L.O. Höglund, Modelling of long-term concrete degradation processes in the Swedish SFR repository, SKB Technical Report R-01-08, Swedish Nuclear Fuel and Waste Management Company, 2001.

[79] A. Babaahmadi, Developement of a method for accelerated ageing of cementitious materials used in repositories of nuclear waste, ISSN 1652-9146, Civil and Environmental Engineering, Chalmers University of Technology, 2013.

[80] Z. Abbas, E. Ahlberg, S. Nordholm, Monte Carlo Simulations of Salt Solutions: Exploring the Validity of Primitive Models, The Journal of Physical Chemistry B, 113 (2009) 5905-5916.

[81] J. Crank, The mathematics of diffusion, Oxford science publications1916.

[82] R. Torrent, Non-Destructive Evaluation of the Penetrability and Thickness of the Concrete Cover - State-of-the-Art Report of RILEM Technical Committee 189-NEC, 2007.

[83] J.J. Kollek, The determination of the permeability of concrete to oxygen by the Cembureau method—a recommendation, Materials and Structures, 22 (1989) 225-230.

[84] ASTM C496/C496M-11, Standard Test Method for Splitting Tensile Strength of Cylindrical Concrete Specimens.

[85] ASTM C39/C39M-14a, Standard Test Method for Compressive Strength of Cylindrical Concrete Specimens.

[86] ASTM C215-08, Standard Test Method for Fundamental Transverse, Longitudinal, and Torsional Resonant Frequencies of Concrete Specimens.

[87] Q. Zhang, G. Ye, Dehydration kinetics of Portland cement paste at high temperature, J Therm Anal Calorim, 110 (2012) 153-158.

[88] P. Faucon, F. Adenot, M. Jorda, R. Cabrillac, Behaviour of crystallised phases of Portland cement upon water attack, Materials and Structures, 30 (1997) 480-485.

[89] J.J. Chen, J.J. Thomas, H.M. Jennings, Decalcification shrinkage of cement paste, Cement and Concrete Research, 36 (2006) 801-809.

[90] A. Rawal, B.J. Smith, G.L. Athens, C.L. Edwards, L. Roberts, V. Gupta, B.F. Chmelka, Molecular silicate and aluminate species in anhydrous and hydrated cements, Journal of the American Chemical Society, 132 (2010) 7321-7337.

[91] K. Haga, M. Shibata, M. Hironaga, S. Tanaka, S. Nagasaki, Silicate Anion Structural Change in Calcium Silicate Hydrate Gel on Dissolution of Hydrated Cement, Journal of NUCLEAR SCIENCE and TECHNOLOGY, 39 (2002) 540-547.

[92] G. Fagerlund, Determination of pore-size distribution from freezing-point depression, Matériaux et Constructions, 6 (1973) 215-225.

[93] B. Johannesson, Dimensional and ice content changes of hardened concrete at different freezing and thawing temperatures, Cement and Concrete Composites, 32 (2010) 73-83.

[94] D.H. Bager, E.J. Sellevold, Ice formation in hardened cement paste, part III - Slow resaturation of room temperature cured pastes, Cement and Concrete Research, 17 (1987) 1-11.

[95] B.M. Braun, H. Weingaertner, Accurate self-diffusion coefficients of lithium(1+), sodium(1+), and cesium(1+) ions in aqueous alkali metal halide solutions from NMR spin-echo experiments, The Journal of Physical Chemistry, 92 (1988) 1342-1346.